PRODUCT DEVELOPMENT PROCESS USING DOUBLE DIAMOND MODEL: A CASE STUDY OF HAMMERMILL SHREDDER TIE BOLTS

Lappeenranta–Lahti University of Technology LUT

Master's Programme in Industrial Design Engineering, Master's thesis 2023

Eero Palmroth

Examiners: Professor Juha Varis, D.Sc. (Tech.)

Amir Togiani, D.Sc. (Tech.)

Supervisor: Tapio Väli-Torala

ABSTRACT

Lappeenranta–Lahti University of Technology LUT

LUT School of Energy Systems

Mechanical Engineering

Eero Palmroth

Product development process using double diamond model: a case study of hammermill shredder tie bolts

Master's thesis

2023

66 pages, 25 figures, 6 tables and 2 appendices

Examiners: Professor Juha Varis, D.Sc. (Tech.) and Amir Togiani, D.Sc. (Tech.)

Keywords: Metal Recycling, Shredding Plant, Shredder, Rotor, Pretension, VDI 2230, Double Diamond

The aim of this research is to conduct product development of hammermill shredder tie bolts using interviews, sample studies, analyses and principles of Double Diamond process methodology. The Double Diamond is two phased process model which is used to identify and define the most problematic areas for improvement and to guide the development of solutions along with literature sources. During initial phase of the research fatigue was discovered as a likely cause for failures in normal conditions and in the second phase possible solutions for improving fatigue life and overall reliability of tie bolts were developed with guideline from VDI 2230 standard by considering changes to tie bolt design, rotor design and bolt material choice.

Proposed solutions included design change in rotor and thread geometry. A prototype tie bolt head was manufactured with a thread larger root radius and it along with rotor design changes were studied using Finite Element Analysis, which suggest that the location of the tie bolts and design change in rotor geometry can offer notable improvement to overall stiffness of the rotor which results in lowered overall stresses in tie bolts. Thread analyses suggest that larger root radius lowered principal stresses at thread root but had limited effect on shear stresses.

The proposed solutions can be considered promising preliminary results in the overall process of product development tie bolt. More information is still required on the causes of breaks as there are possibly many contributing factors such as corrosion. With the available data obtained during the research the totality of their effect on tie bolt failures couldn't be judged with certainty.

TIIVISTELMÄ

Lappeenrannan–Lahden teknillinen yliopisto LUT

LUT Energiajärjestelmät

Konetekniikka

Eero Palmroth

Tuotekehitysprosessi käyttäen Double Diamond -mallia; tutkimustapaus vasaramurskan roottorin sideruuveista

Konetekniikan Diplomityö

2023

66 sivua, 25 kuvaa, 6 taulukkoa ja 2 liitettä

Tarkastajat: Professori Juha Varis, TkT ja Amir Togiani, TkT

Ohjaaja: Tapio Väli-Torala

Avainsanat: Metallien kierrätys, Murskaamo, Vasaramurska, Roottori, Esikiristys, VDI 2230, Double Diamond -malli

Tämän tutkimus keskittyi vasaramurskan roottorin sideruuvien tuotekehitykseen käyttäen haastatteluja, näytetutkimuksia, analyysejä ja Double Diamond -mallin periaatteita. Double Diamond on kaksiosainen prosessimalli, jota käytettiin kehityskohteiden määrittelyyn ja ohjaamaan tuotekehitystä kirjallisuuslähteiden mukana. Ensimmäisessä tutkimusvaiheessa väsyminen osoittautui todennäköiseksi vauriomekaniikaksi normaalissa käytössä ja toisessa tutkimusvaiheessa mahdollisia ratkaisuja väsymiskestävyyden ja sideruuviliitoksen luotettavuuden lisäämiseen kehitettiin VDI 2230 standardin ohjeiden mukaisesti tutkimalla mahdollisuuksia muutoksiin sideruuvien ja roottorin rakenteessa sekä mahdollisissa materiaalivaihtoehdoissa.

Ehdotetut ratkaisut liittyvät kierteeseen ja roottorin rakenteeseen. Tutkimuksen aikana prototyyppi isomman kierteen pohjan omaavasta kierteestä valmistettiin ja sen sekä roottorirakenteen muutoksien vaikutusta tutkittiin elementtimenetelmän analyysein. Tutkimus osoitti roottorirakenteen muutoksen lisäävän roottorin jäykkyyttä, joka alensi sideruuvien jännityksiä kuormituksessa. Kierteen pohjan analyysi osoitti, että suurempi pohjasäde alensi pääjännityksiä kierteen pohjalla, mutta vaikutus oli rajallinen leikkausjännitysten osalta.

Ehdotettuja ratkaisuja voidaan pitää lupaavina alustavina tuloksina sideruuvien tuotekehityksessä. Lisää tietoa kuitenkin tarvitaan muista negatiivisesti vaikuttavista tekijöistä kuten korroosiosta, joiden vaikutusta sideruuvien rikkoihin ei tutkimuksen aikana saadulla tiedolla voitu riittävän tarkkaan määritellä.

ACKNOWLEDGEMENTS

I would like to thank my supervisors Tapio Väli-Torala and Ville Rautiola and my colleague Pekka Vainio at RecTec Engineering for interesting subject and support during this study. I also highly valued the comments and experiences shared by my examiners Juha Varis and Amir Togiani as well as the many people within the recycling industry who are too numerous to mention.

Above all the biggest thanks goes to my wife Inka and my son Toni for their love, hugs and tireless patience over the course of my studies.

Eero Palmroth

Heinolassa 10.6.2023

SYMBOLS AND ABBREVIATIONS

Note on the decimal separation punction marks used with numbers

Data presented in some of the figures are taken from programs that use commas as decimal separator instead of dots, therefore, the commas “,” in figures and tables should be interpreted as dots “.” when looking at the presented values and results.

Roman characters

A_{Red}	Cross-sectional area of equivalent cylinder [mm²]
A_S	Tensile stress area of the bolt [mm²]
BL_a	Bolt load at when joint is under load of a
BL_b	Bolt load at when joint is under load of b
BL_{pa}	Bolt load when preloaded and joint is under load of a
BL_{pb}	Bolt load when preloaded and joint is under load of b
d	Basic major diameter of external thread [mm]
D	Basic major diameter of internal thread [mm]
d_1	Basic minor diameter of external thread [mm]
D_1	Basic minor diameter of internal thread [mm]
d_2	Basic pitch diameter of external thread [mm]
D_2	Basic pitch diameter of internal thread [mm]
D_A	Outer dimension of the equivalent cylinder [mm]
D_B	Diameter of the bolt hole [mm]
d_K	Diameter of the bearing surface of the bolt or nut [mm]
D_{km}	The average diameter of the circle of friction [mm]

E	Modulus of Elasticity [Pa]
F	Force [N]
F_B	Tensile force acting on bolt [N]
F_{Bmax}	Maximum clamping force [N]
F_{Bmin}	Minimum clamping force [N]
F_M	Axial force obtained during assembly from detailed equation [Nmm]
F_{CL}	Compressive force on joint [N]
g	Gravitational acceleration 9,81 m/s
H	Height of fundamental triangle in ISO 68 thread [mm]
JL_0	Joint load at zero
JL_a	Joint under load of a
JL_b	Joint under load of b
K	Coefficient often referred to as Nut Factor with a typical value of 0.2
K_B	Spring constant of the bolt or different portions of the bolt
K_J	Spring constant of compressed parts
K_N	Spring constant of the nut
K_T	Total spring constant of the bolted connection
K_W	Spring constants of the washers
L_0	Initial length of the bolt
Le	Effective length of the bolt [mm]
l_K	Combined thickness of the clamped parts [mm]
L_X	External force acting on bolted connection [N]
L_{XCrit}	Critical external force [N]
m	Mass [kg]

M_A	Torque during assembly from detailed equation
n	Load plane factor
P	Thread pitch [mm]
PL_0	Bolt preload at zero
PL_1	Bolt preload at level one
r	Radius [mm]
R_e	Yield strength [MPa]
R_{eB}	Yield strength of a bolt [MPa]
R_m	Tensile strength [MPa]
R_{mB}	Tensile strength of a bolt [MPa]
R_{Root}	Root radius of thread [mm]
s	Estimated scatter [%]
T	Torque during assembly from general equation
v_p	Utilization level of bolt's yield strength with typical maximum value of 0.9
x	Dimensionless constant

Greek characters

α	Material specific coefficient of thermal expansion [1/C°]
αA	Coefficient of Scatter during preloading
ΔF_J	Change in clamping force from the external force
ΔF_P	Change in clamping force from relaxation and elastic interactions
ΔF_{Prqd}	Minimum clamping force requirement for a joint
ΔL	Elongation of the bolt
Δl_K	Change in thickness of the clamped parts

ΔT	Change in temperature
Φ_K	Load factor
σA	Endurance Limit
σ_B	Tensile stress on the bolt [MPa]
μ_G	Frictional coefficient between mating threads
μ_K	Frictional coefficient between mating surfaces
ω	Angular velocity [1/s]

Superscripts

"	inch

Abbreviations

ASR	Automotive Shredder Residue
CAD	Computer-aided design
CAE	Computer-aided engineering
DIN	German institute for Standardization
EOL	End-of-life
FE	Ferrous metals
FEA	Finite Element Analysis
ISO	International Organization for Standardization
M	Metric 60° flank angle thread system based in millimetres
NF	Non-ferrous metals
Q&T	Quenched and Tempered condition
SSC	Stress Corrosion Cracking

SLF	Shredder Light Fraction
UN	Unified 60° flank angle thread system based in inches
VDI	Verein Deutcher Ingenieure, the German society of engineers

Table of contents

Abstract

Acknowledgements

Symbols and abbreviations

1 Introduction 10
1.1 Background of the research 11
1.1.1 Research problem and research questions 11
1.2 Goals of the research 11
1.3 Scope and limitations of the research 11
1.4 Previous research on the topic 12
1.5 Recycling of EOL-vehicles 12
1.6 Automotive hammermill shredders 13
1.7 Shredder rotors 16
1.7.1 Rotor dynamics and balance 17
2 Shredder rotor tie bolts 19
2.1 Metric threads 20
2.1.1 Metric thread tolerances 22
2.2 Bolted connections 22
2.2.1 Failures in bolted connections 23
2.2.2 Fatigue in bolted connections 23
2.2.3 Corrosion in bolted connections 25
2.3 Parts of a bolted connection and calculation of pretension 26
2.3.1 Stiffness of parts in a bolted connection 26
2.3.2 Joint diagrams 29
2.3.3 The effect of lubrication 30
2.3.4 The effect of thread pitch 31
2.3.5 General application of preload 31
2.3.1 Preload calculation process 33
2.3.2 Tension equations 35

3 Methods 39
3.1 Double Diamond process model 39
3.2 Interviews with shredder operators 41
3.3 Study of the samples 41
3.3.1 Objective and method study with the samples 42
3.4 Prototypes and Finite Element Analyses 42
3.4.1 FEA of bolts within rotor geometry 42
3.4.2 FEA of bolt thread geometry 45
4 Results 48
4.1 User experiences of shredder operators 48
4.1.1 Insights from the operator interviews 49
4.2 Study of bolt samples 50
4.2.1 Insights from the sample studies 50
4.3 FEA of rotor design 54
4.4 FEA of thread root geometry 56
4.5 Tie bolt materials 57
4.6 Analysis of the FEA results and collected data 59
5 Discussion 60
6 Conclusions and summary 62
References 64

Appendices

Appendix 1. Questionnaires

Appendix 2. Calculation model for rotor analysis

1 Introduction

In recycling, the material comminution has always been an essential part of processing. A working comminution is often the first step that ensures the different materials in products can be separated in subsequent processes. Different shredders and mills are commonly used as the machines to accomplish this process, and they vary broadly from small machines used in sample crushing to large hammermill shredders that are used to process mixed metal scrap and end-of-life (EOL) vehicles.

In a hammermill shredder, the comminution happens when material fed into the shredder where it is hit repeatedly by the swinging hammers attached to the shredder rotor. The hammer impacts tear pieces from the material and the pieces stay within the shredder until they are small enough to fit through the shredder grating. The process is energy intensive and many parts experience high forces and severe wear during normal operation, which means shredders normal operation requires constant monitoring and regular inspections and maintenance.

This research which is commissioned by RecTec Engineering Oy focuses on product development of tie bolts in disk-type hammermill rotors. A tie bolt is a long stud bolt in the shredder's rotor which are used to tighten the disks during assembly and add stiffness and stability to the rotor during operation. The research consists of introductory part which includes overview of the background and goals of the thesis, as well as review of previous studies that have examined bolt failures. A brief overview metal recycling industry and the different hammermill shredder rotor constructions are also included, as well as bolt design and failure theory.

Both qualitative methods such as interviews and quantitative methods such as measuring and studying of used bolts and simulating the possible solutions using computer-aided engineering (CAE) software are used during the research. Principles of Design Thinking methodology, which emphasize human-centred design and inclusion of stakeholders in the design process, are also used by employing the Double Diamond process model, where the analysis and synthesis stages follow each other in iterative manner to produce the desired outcome.

1.1 Background of the research

The background of the research stems from the repeated maintenance operations made to rotors when a tie bolt has failed during operation. A single broken bolt doesn't immediately lead to catastrophic failure, but the shredder operators often have a strict maintenance policy where bolt failures are either immediately fixed on site or the rotor is switched with a replacement and serviced later. In both methods the shredder operator faces some downtime, and a single bolt failure might lead to switching of all the tie bolts as a precautionary measure which adds costs and material use.

1.1.1 Research problem and research questions

The research problem is identifying the factors that currently hinder tie bolt's service life and find improvement areas in order to enhance it. The main research question is: What is the reason and the primary mechanic of tie bolt failure? Secondary research question is what is the optimal pretension for tie bolts?

1.2 Goals of the research

The main goal of this study is to update the design guidelines and present the optimal design parameters for tie bolts with respect to the expected loading conditions and improve the general service live of tie bolts.

1.3 Scope and limitations of the research

The scope of this study is limited to improving the initial service life of tie bolts and aspects of possible in situ repairs or other maintenance after bolt failures are not specifically studied. In the study is also limited to suggested solutions and simulations as in practice verifying the improvement in service life will in take several years of monitoring.

1.4 Previous research on the topic

There aren’t any public research dealing with shredder tie bolts in particular, but there are several standards and technical literature dealing with bolts and bolted joints in general. The VDI 2230 standard (2015) by German society of engineers Verein Deutcher Ingenieure (VDI) in particular is referred in several literature sources and the methodology described in it has been widely used in design of bolted joints. There are also studies that deal with bolt failures and their analyses such as a study by Hyvönen (2021) about bolt fatigue strength in pulsating compressive stress. In his study he suggested possible areas for improvements to fatigue strength by modifications to thread geometry, preload and if possible to joint structure, which concurs with the general recommendations found from literature.

1.5 Recycling of EOL-vehicles

Recycling to separate different metals from scrap is one of the oldest and most established branches of recycling. Metals in general have many good properties for recycling due to their ability to retain quality in re-processing and excellent response to different separation technologies such as magnetism, electromagnetic induction, and density-based classification. By material composition a classic example of metals recycling is the recycling of EOL-vehicles, which by weight contain an average 75.5% of different metals. (Suomen Autokierrätys Oy, nd).

Basic process of EOL-vehicles recycling consists of pre-processing where the liquids, tyres, batteries, and any other hazardous parts are removed. During this phase also any easy to remove valuable parts such as catalytic converters or parts that can be used as spares are removed before the rest of the car is processed by the shredder. In addition to EOL-vehicles the shredder plants usually process other types of metal scrap as well such as electric appliances, consumer white goods, or other mixed metal scrap.

A shredding facility usually consists of a feed system such as a chain belt conveyor or hydraulically operated slope that is used to transport the scrap into the shredder. The shredded material is then moved by a conveyor system into air classifier that separates the Shredder Light Fraction (SLF) from metals and other heavier materials, which are then subsequently separated into ferrous metals (FE) from non-ferrous (NF) by magnet drums

and eddy current separators, with the final portion of the initially shredded material forming a heterogenous mixture of different materials with only trace amounts of metals known as the Automotive Shredder Residue (ASR). Shredding of material produces lot of particles and dust emissions which are controlled either by particle removal though a combination of a cyclone paired with either a wet scrubber or a filter, or by introducing water into the shredder in a controlled manner. An example of a basic layout of a shredding facility with emissions removal through a cyclone and filter combination can be seen in figure 1.

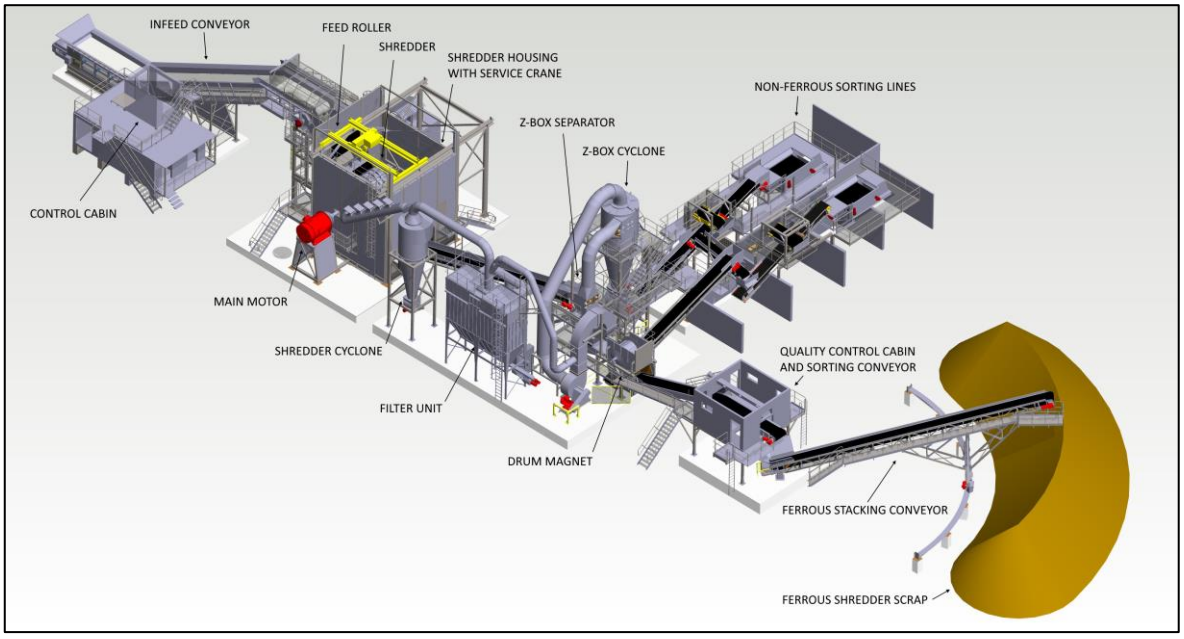

Figure 1. An example of a basic layout of a shredding facility with initial SLF separation through Z-Box air classifier and perpendicularly separated lines for FE and NF materials.

1.6 Automotive hammermill shredders

The shredders used in processing of EOL-vehicles are predominantly high-speed hammermill shredders that in general work with the same principles introduced during the first generations of commercial automobile hammermill shredders dating from late 1950s to 1960s. Some of the landmark machines of the industry such as the Newell Shredders shown in figure 2 created in the following decades can be found in operation even today. Shredders

are often classified by a number combination, where initial digits mark the maximum diameter of the hammer swing and next digits the internal width of the shredder anvil or the throat.

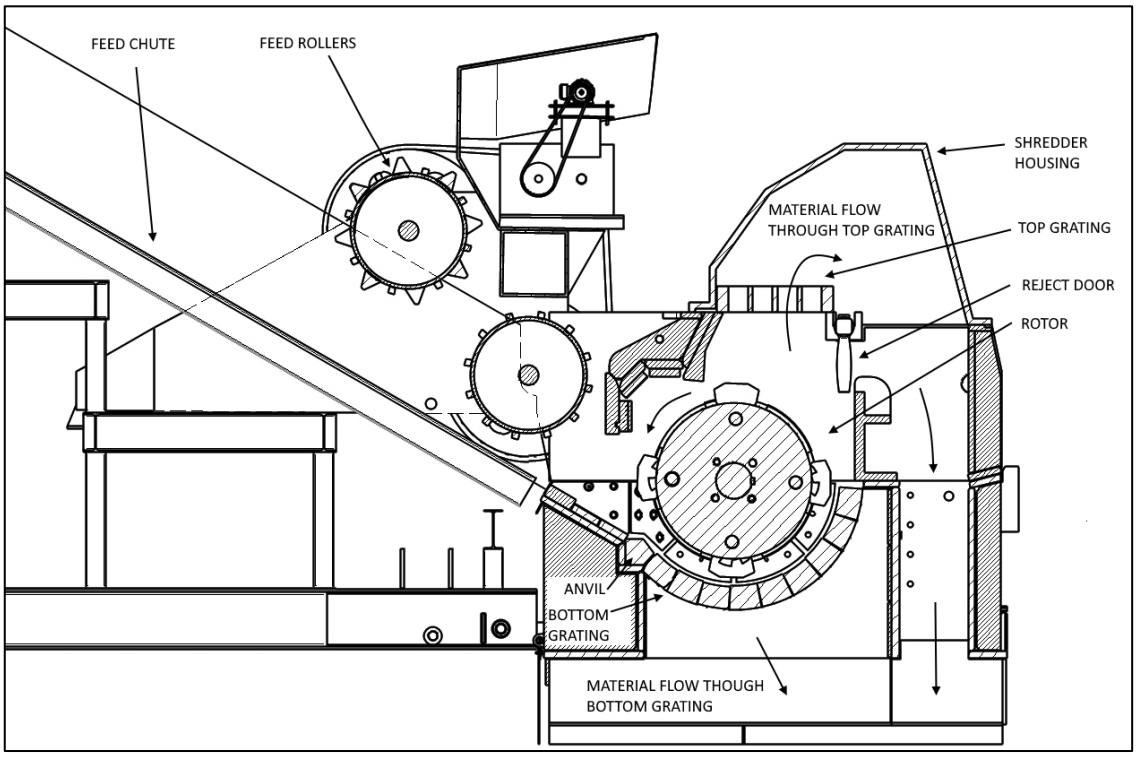

Figure 2. Newell hammermill shredder (modified from ASME 1994).

The basic principle of current shredders is to load the scrap into the shredder by inclined plane and control the material feed through feed rollers. The scrap that enters the shredder is impacted by the rotating hammers against the bottom anvil located in mouth of the shredder. The impacts from hammers and the resulting collisions begin to comminute the material until it is broken down and deformed to sufficiently small pieces that can exit the shredder either through top or bottom grating. The hammers are free to move around, and if a piece of scrap fails to break from the impact, the hammer can rotate back, and quickly return to the extended position due to the effect of centrifugal forces. Pieces that are too large or tough to be broken, commonly known as unshreddables, typically move through the shredder into the space above the rotor where the reject door can be opened to allow these objects to exit the shredder. Typical unshreddable items include large diameter shafts, axles or rebars,

heavy plates, and large diameter structural shapes. (ASME 1994; Nijkerk & Dalmjin 2004, p. 93-94)

Shredder housing is composed of very robust bottom and top parts, which are always protected by replaceable wear plates. The top part can be opened by hydraulic cylinders to enable periodic maintenance operations, which include visual inspections, bolt tightness checks, hammer, and wear plate changes, and in some cases resurfacing or repairing of the rotor disks though welding. More detailed view of the different parts in shredder can be seen in figure 3, which contains a section view of an example bottom discharge hammermill shredder. (Nijkerk & Dalmjin 2004, p. 95)

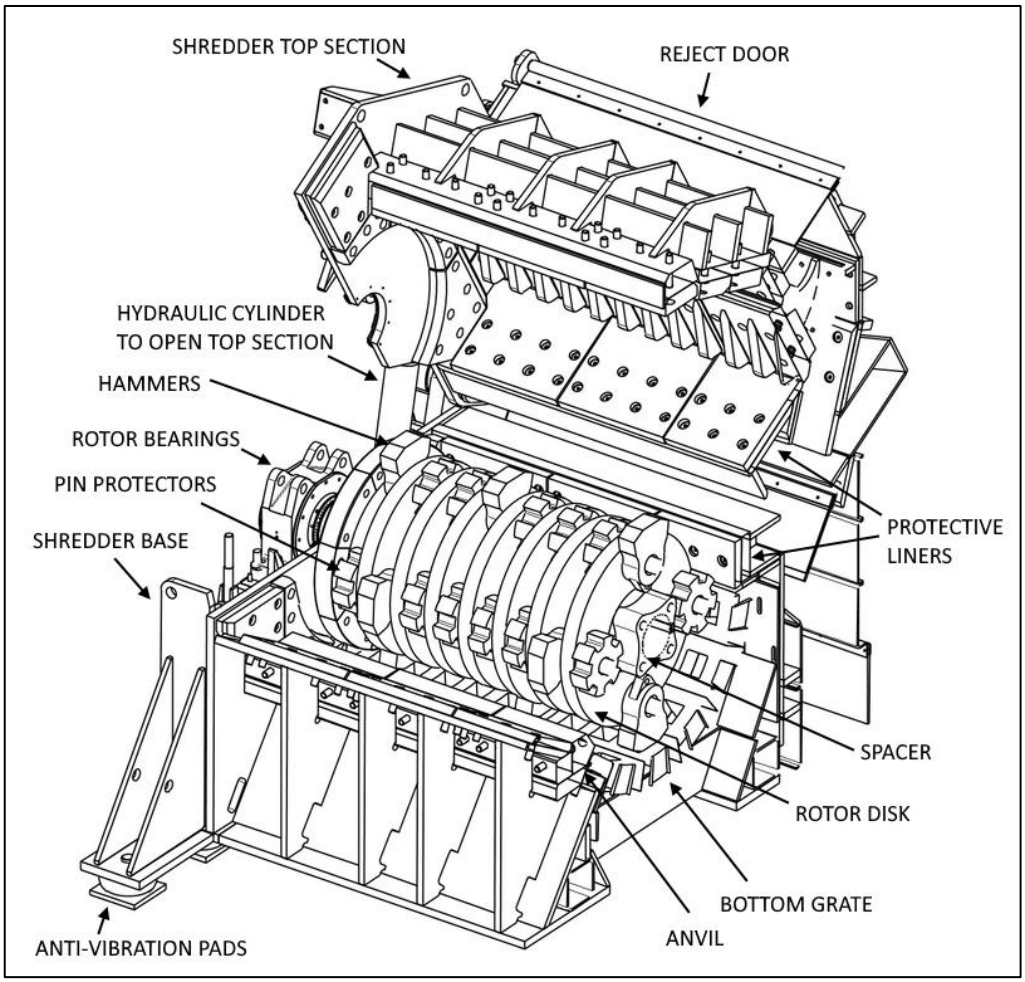

Figure 3. Section sketch of an example bottom discharge hammermill shredder.

1.7 Shredder rotors

Hammermill shredder rotors generally fall in to two categories, welded or capped disk rotors and spider rotors. Disk rotors consists of several disks separated by spacers that are connected to a heavy shaft by one or more keys. The disks and spacers, which are usually made from wear resistant material, are heat shrunk in place and tightened together by tie bolts that run through the entire rotor. The hammers, which are typically manganese steel castings, are connected to axles located in the outer rim of the disks. The axles, often referred to as hammer pins, provide different places along the rotor where hammers can be placed to spread out the wear and allow the use of different hammer patterns and configurations. All of the pin locations without a hammer are covered with protective manganese steel castings to ensure maximum lifespan for the hammer pins. An example of a disk rotor can be seen figure 4. (ASME 1994; Nijkerk & Dalmjin 2004, p. 102-103)

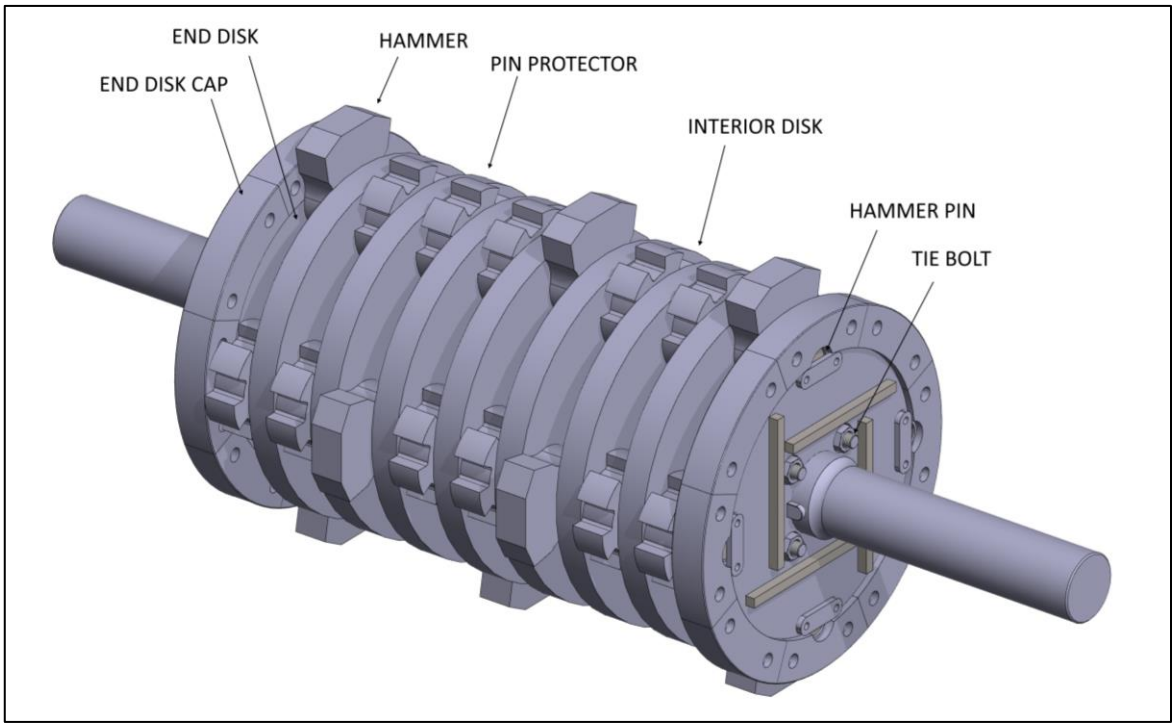

Figure 4. An example of a disk rotor.

The rotor discs themselves don't actively crush the material, but they suffer from a general wear which is typically countered by an abrasion resistant material choice and a periodically re-welded hardfacing. Disk rotors can also have protective caps placed around the outer edge of the disks and a fully protected rotor is often referred to as a barrel rotor. A spider rotor shares all the same principles as disk rotors but differs in construction as it doesn't have spacers and instead has a distinct arm-like geometry where inner plates are stacked in an angle to each other to create the gaps where hammers can rotate, and pin protectors be placed. (Nijkerk & Dalmjin 2004, p. 96)

1.7.1 Rotor dynamics and balance

Overall balance of shredder rotor is essential hammermills due to the high rotational velocity. The rotational speed depends on the size of the hammer swing diameter, where the goal is often to have speeds of 60-70 m/s at the hammer tip. This often translates to speeds of 720-750 rounds per minute (RPM) on smaller rotors and 500-600 RPM on larger diameter rotors.

The main cause of imbalance to the rotor is the overall wear, which is most evident at the hammers, and therefore their placement around the rotor is strictly governed by balance. This means that there needs to be equal number of hammers spread across the rotor to minimize imbalance, with some variations possible usually depending on the total amount of hammers. These variations, often referred to as hammer patterns, are usually different arrowlike forms with the purpose of driving the material from sides of the shredder to the center. Balance is also an important consideration during maintenance where for instance if a hammer is changed, or local resurfacing done, the opposite side must also be attended to retain the overall balance. Free body diagram of the basic dynamic model of a disk rotor can be seen in figure 5, where line between bearings *A&B* represents the rotor's axis of rotation, points *H* the locations of the hammers and ω the angular velocity which affects the centrifugal forces acting at each hammer according to formula:

$$F = mr\omega^2 \tag{1}$$

Where *m* equals the mass of the hammer and *r* the distance to its center of mass from the axis of rotation.

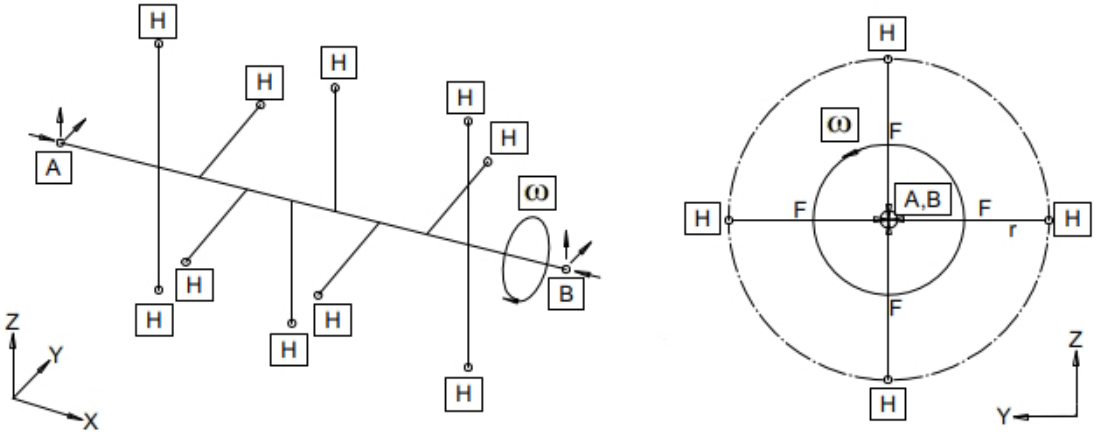

Figure 5. Free body diagram of the basic dynamic model of a disk rotor.

It can be seen that the balance of masses at the rotor's outer edge should remain as equal as possible to minimize imbalance loads that the bearings must counteract. In addition to overall balance an important factor in rotor dynamics is the overall bending stiffness of the rotor which is increased by the effect of tie bolt clamped rotor disks.

2 Shredder rotor tie bolts

Rotor tie bolts are essentially a set of long stud bolts that are used to tighten the rotor assembly together and increase the overall stiffness of the rotor. The amount of tie bolts in a rotor assembly usually equals the amount of hammer pins, thus four tie bolts in smaller rotors and six or more in larger constructions. The tie bolts are usually made from high strength Medium Carbon alloy steel such as 42CrMo4 that is heat-treated to Quenched and Tempered (Q&T) condition and have Metric (M) or Unified (UN) 60° flank angle threads in both ends. Example setup of tie bolts in a disk rotor and a dimensional drawing of a tie bolt can be seen in figures 6 and 7. The sample geometry roughly conforms to a rotor with a hammer swing radius of 1500 mm and anvil width of 2250 mm or 60” by 90” inches.

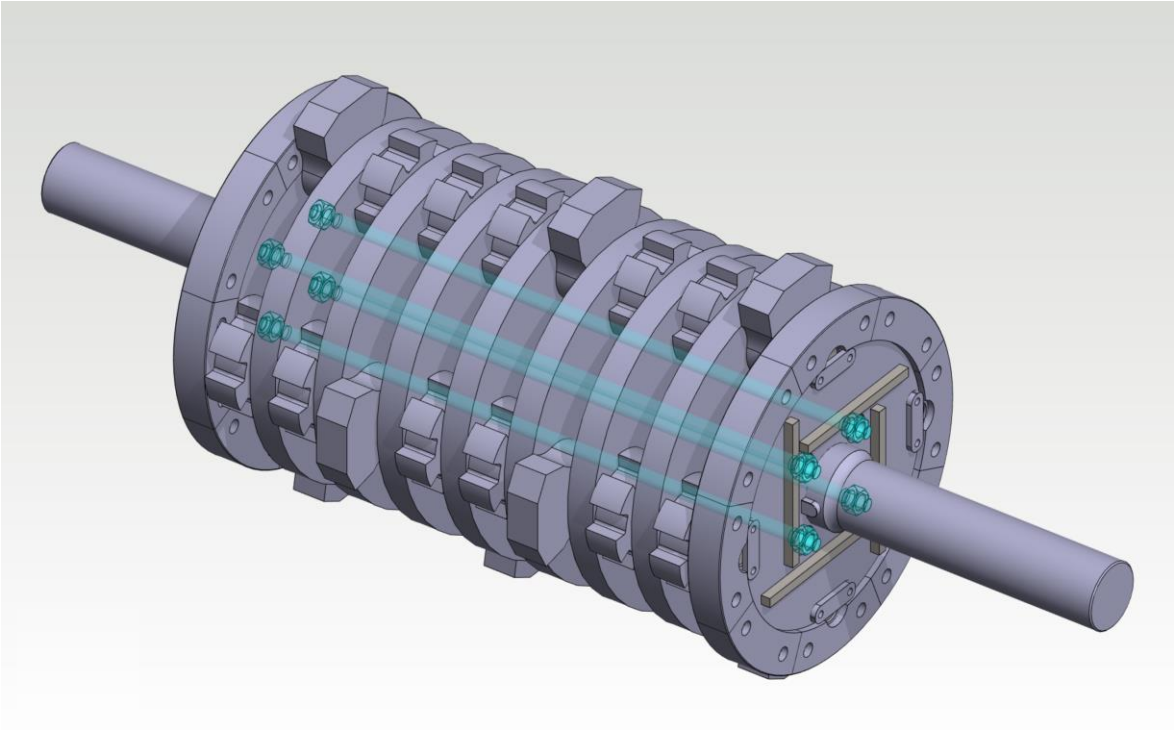

Figure 6. Tie bolts highlighted on the disk rotor example.

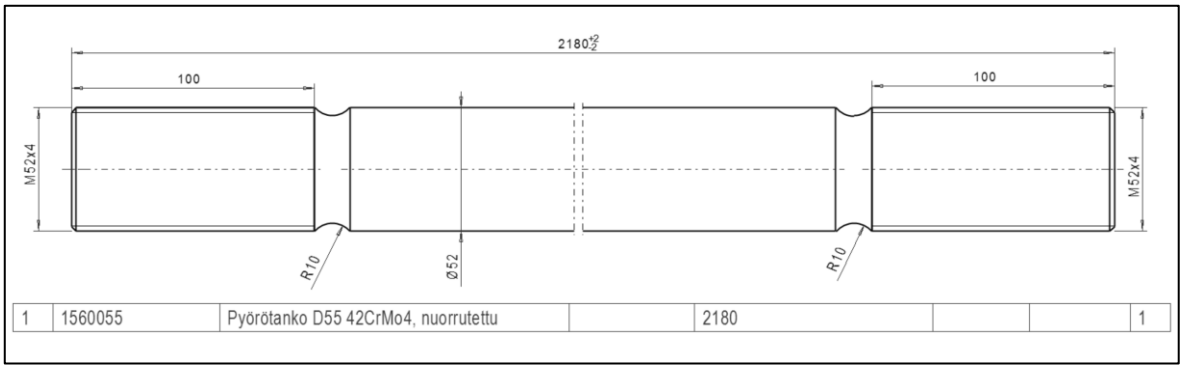

Figure 7. Measurements and material data of tie bolts on the disk rotor example.

2.1 Metric threads

60° flank angle is most commonly used thread form in fasteners around the world, with metric and imperial measurement systems having their own M and UN systems respectively. The basic profile for ISO 68 metric threads can be seen in figure 8.

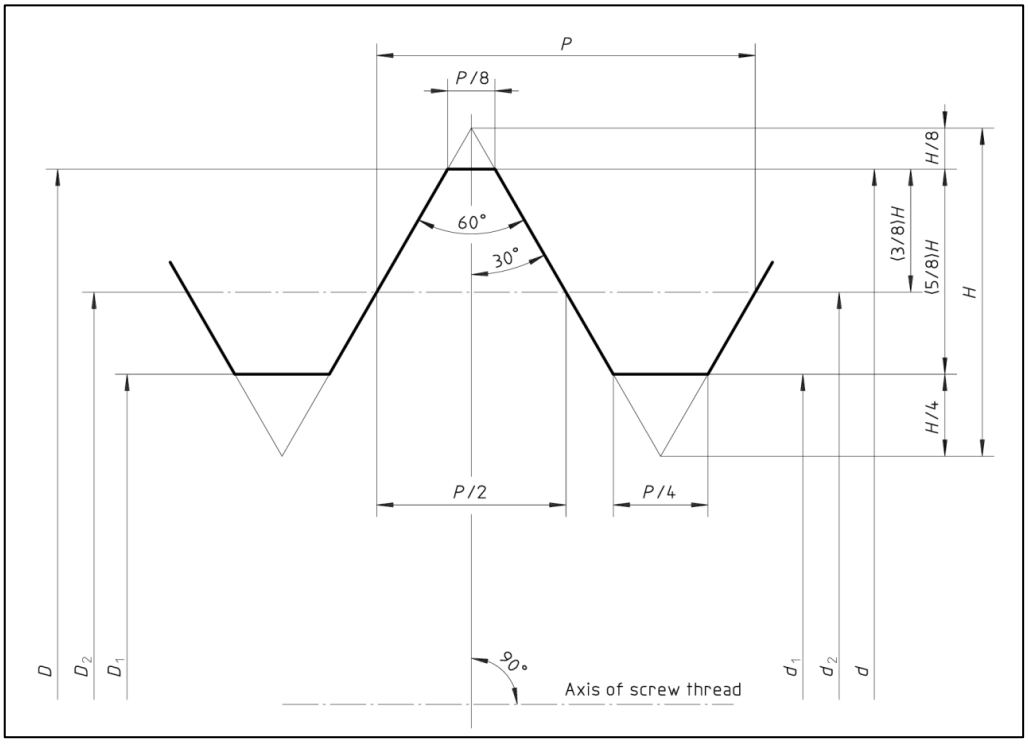

Figure 8. Metric thread profile as defined in ISO 68 standard (SFS-ISO 68-1 2010).

where

P = Pitch of the thread

H= The height of the fundamental triangle

D,d = The basic major diameters

D_2, d_2 = The basic pitch diameters

D_1, d_1 = The basic minor diameters

The main dimensions of the fundamental triangle can be expressed in through pitch as shown in the equations 2-6 below.

$$H = \frac{\sqrt{3}}{2} \times P = 0{,}866025404 \times P \quad (2)$$

$$\frac{5}{8}H = 0{,}541265877 \times P \quad (3)$$

$$\frac{3}{8}H = 0{,}324759526 \times P \quad (4)$$

$$\frac{H}{4} = 0{,}216506351 \times P \quad (5)$$

$$\frac{H}{8} = 0{,}108253175 \times P \quad (6)$$

The thread profiles are categorized by the pitch as coarse or fine, where coarse pitch is considered as default choice used in general applications and fine threads in more specialized applications where for instance increased strength is required from the joint or length of engagement with the mating threads is too small to accommodate coarse threads. The increased strength of finer threads is directly related to the increase in cross sectional area due to the thread geometry as the fundamental triangle of smaller pitch requires less material removal towards axis of the thread resulting in larger minor diameter. Preferred metric thread choices for general design work in SFS-ISO 262 (2010) standard, which covers diameters from 1 - 64 mm.

2.1.1 Metric thread tolerances

Metric thread tolerances are covered SFS-ISO 965-1 (2019) standard. Thread tolerance markings indicate the tolerance position and grade with respect to zero line as seen in figure 9, where the letter marks the fundamental deviation and numeric tolerance grade the amount of tolerance, which always adds to the gap between mating surfaces. The most common combination is the *6g/6H* tolerance, which indicates a tolerance by a grade of *6* on both external bolt thread and internal nut thread, and slightly negative fundamental deviation on external thread indicated by position *g* and no fundamental deviation on internal thread indicated by position *H*. Standardized tolerance grades are available for pitch and minor diameters of internal thread as well as pitch and major diameters of external threads.

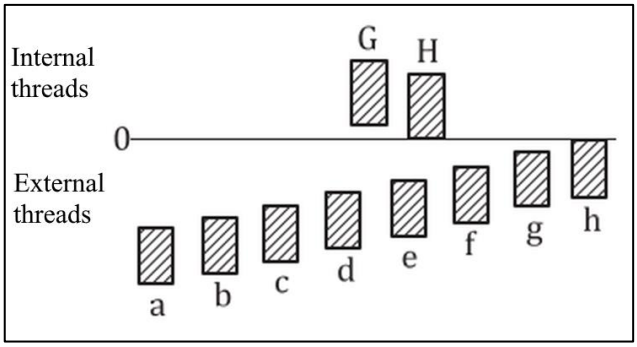

Figure 9. Tolerance positions of internal and external metric threads (modified from SFS-ISO 965-1 2019, p7.)

2.2 Bolted connections

Bolted connections in general are categorized by the way they transmit forces. In shear connections the transmitted forces are perpendicular to the axis of the bolt and in tension connections the transmitted loads are parallel to the axis of the bolt. In addition to the transmit of forces bolted connections follow important distinction and different design principles depending on the type of loading the connection is subject to. When the magnitude or direction of load varies over time or is cyclic the connection is considered dynamically

loaded and in addition to tensile overload can also fail through fatigue. (Bickford 2008, p. 1-2, 327)

The concept of preload is an essential part of dynamically loaded connections. A bolted connection where the bolt is pretensioned is usually referred to as loaded, and it's one of main design requirements is to keep the connected surfaces in compression and prevent their movement, which is often referred to as slipping. In context of machine design slipping of dynamically loaded connection can result in several problems such as leaking, fatigue, fretting corrosion or loosening of the joint. In structural steel construction, shear connections with loaded joints are common and they are referred as slip-resistant or slip-critical connections, which are normally designed to transmit forces with friction between clamped surfaces but can fail with a degree of safety by a controlled slip and revert into a shear connection in case an overload. (Bickford 2008, p. 3; Airila et al. 2010, p. 225-226)

2.2.1 Failures in bolted connections

Bolted connection can suffer failures in several ways. According to Bickford (2008, p.6) critical failures include fractures or thread stripping in bolt or nut due to overload or fatigue, failures in connected parts if they yield under load or bolt or nut shears through and loosening of the joint due to vibration. As failures are usually also considered instances where overload of the joint results in permanent deformations or initial preload fails to maintain clamping force during in service conditions, although in either case the failure doesn't necessarily immediately lead to a critical failure.

2.2.2 Fatigue in bolted connections

Fatigue failures are common issue in bolted connections that are subjected to dynamic tensile loads. A fatigue failure follows the sequence of crack initiation starting at a point of stress concentration or a defect followed by initially slow growth phase that eventually accelerates to a point where final fracture happens instantly after a sufficiently large load. Stress levels leading to fatigue failure can be well below materials tensile limits and more important consideration when assessing fatigue life is the mean stress level and in particular the stress

amplitude, which is the difference between maximum stress and mean stress of dynamic load. (Bickford 2008, p. 327-328)

The basic premise of estimating fatigue life of a part is to compare its endurance limit or fatigue strength against the stress amplitude, where the endurance limit presents the level of alternating stress the part can handle indefinitely and the fatigue strength the amount cycles a certain level of stress peaks is expected be needed in order to cause fracture through the normal process of fatigue crack growth to failure. The stress amplitude can be lowered by preloading a connection which is illustrated in figure 10, where changing joint load in an unloaded connection from JL_a to JL_b changes bolt load linearly from BL_a to BL_b, but after applying preload of PL_1 only from BL_{pa} to BL_{pb} which is highly beneficial in terms of fatigue life if it takes the stress amplitude below materials endurance limit or considerably lowers the level of stress peaks even though the mean stress at the bolt stays at a higher level. (Bickford 2008, p. 342-343)

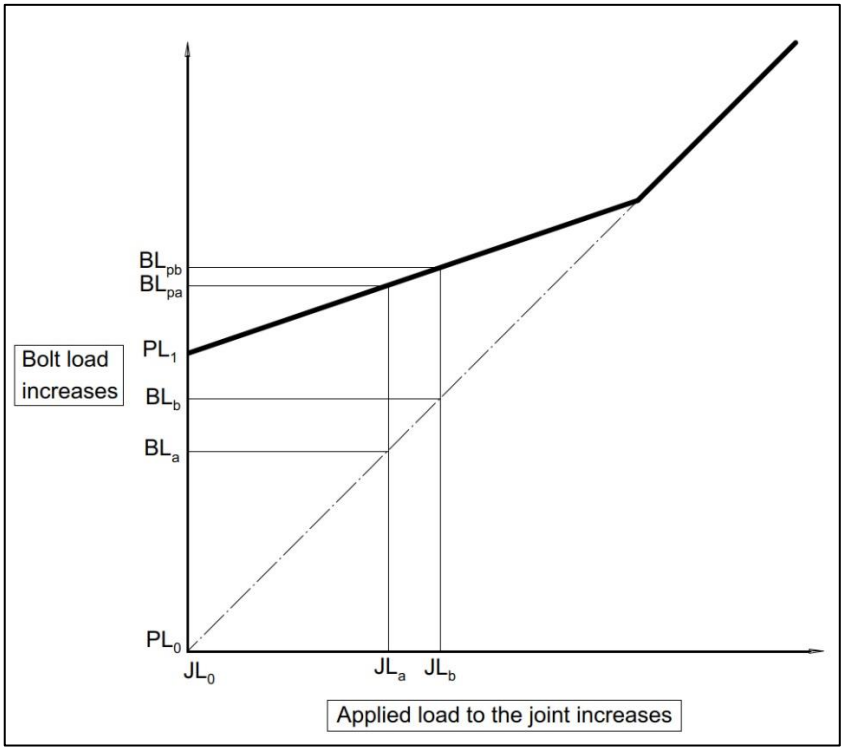

Figure 10. Diagram of preloads effect to bolt load in axially loaded joint (modified from Oberg et al. 2020, p. 1655).

Other factors that have noticeable effect on fatigue strength of a part are its shapes and geometries that act as stress concentrators, overall condition, presence of corrosion and suitability of material. Fatigue performance in general is increased by increasing the tensile strength of the material, but if corrosion or stress concentrators are present, they tend to outweigh the benefit of material change if only it is improved. (Bickford 2008, p. 343-348)

2.2.3 Corrosion in bolted connections

Corrosion presents challenges with many metals, and it can be particularly detrimental in bolted connections when combined with high stresses and presence of dynamic loads. In addition to typical corrosion challenges such as galvanic corrosion the bolted connections can also exhibit fretting corrosion, crevice corrosion and stress corrosion cracking (SSC).

Fretting corrosion is a type of erosion that can happen between loaded contact areas of two metal surfaces, such as the threads, when they are subject to a very slight movement for instance due to vibration. The damage to surfaces starts with local adhesion and continues when particles break apart and react to surrounding environment. The damaged surfaces can show pits or grooves filled with corrosion products. Fretting corrosion is very damaging in terms of fatigue life, but its likelihood can be minimized by methods such as applying sufficient preload, using hard contact surfaces and ensuring good tightness of fit between contacting surfaces. (ASM International 1996, p. 801-809)

Crevice corrosion is a form of localized corrosion located in narrow spaces, which in context of a bolted joint can for instance be located under a nut or bolt head. In there the oxygen within trapped moisture can become depleted, which creates an oxygen differential that turns the moisture acidic and subsequently more anodic than the other material next to it, which starts to corrode the crevice. Suggested solutions to prevent crevice corrosion include designs that eliminate crevices and different protective coatings. (Bickford 2008, p. 359)

SCC is a phenomenon where the concentrated stress at the crack root makes the crack slightly anodic with respect to the other material. In presence of electrolyte such as humidity this creates a tiny galvanic corrosion cell that corrodes the crack and speeds up its growth. Likelihood of problems related to SCC are related to three main causes, which are high stress levels, susceptibility of material and the presence of an electrolyte. High stress levels can for

instance be induced by excessive preload and main material property linked to susceptibility to SCC is high hardness paired with low ductility. (Bickford 2008, p. 363-368)

2.3 Parts of a bolted connection and calculation of pretension

During tensioning bolt acts as a stiff spring that can store potential energy which is transformed into a clamping force within the connection. In assessing the effect and magnitude of preload essential concepts are materials, geometries, and stiffnesses of different parts, the effects of external forces, and accuracy of methods used in pretensioning and predicting the effects of different phenomena that can affect final pretension.

2.3.1 Stiffness of parts in a bolted connection

Stiffness of a part in bolted connection is calculated from the relation of force to a change in length, which usually is the stretch in bolt and compression of the clamped parts. In a simple case the stiffness of a bolt can be approximated simply by substituting the force with product of modulus of elasticity and tensile stress area of the bolt following the equation:

$$K_B = \frac{F_B}{\Delta L} = \frac{EA_S}{L_e} \tag{7}$$

where

K_B = Spring constant of the bolt

F_B = Axial force acting on bolt

ΔL = Change in length

E = Modulus of Elasticity

A_S = Tensile stress area of the bolt

L_e = Effective length of the bolt

The effective length L_e of the bolt is the portion of total length which is under tensile stress. For calculation purposes the effective length can be defined as half of the lengths of bolt head and added to the total length of clamped parts. More detailed calculations can be made if the bolt consists of several distinct sections with different cross-sectional areas, or the connection includes washers, the total combined spring constant can be calculated by adding the spring constants of individual sections together. (Bickford 2008, p.89-92).

$$K_T=(\sum_{B=1}^{n}\frac{1}{K_B}+\sum_{W=1}^{n}\frac{1}{K_W}+\frac{1}{K_N})^{-1} \quad (8)$$

where

K_T = Total spring constant of the bolted connection

K_B = Spring constants of the different portions of the bolt

K_W = Spring constants of the washers

K_N = Spring constant of the nut

In assessing the stiffness of the compressed members their body often can't be expressed as simply and confidently as in case of the bolt. In those cases, the body consisting of compressed members is represented by a suitably equivalent shape such as a cone or a cylinder starting from the faces of the bolt nut heads and expanding towards each other in a manner which best describes the joint. This shape is often called pressure cone or equivalent cylinder, which can be seen in figure 11, and the stiffness of the connected parts in a through bolted connection shown there can be calculated by following equations below when conditions $d_K \leq D_A \leq d_K + l_K$ apply. (Airila et al. 2010, p. 200).

$$K_J=\frac{F_{CL}}{\Delta l_K}=\frac{EA_{Red}}{l_K} \quad (9)$$

$$A_{Red}=\frac{\pi}{4}*(d_K{}^2-D_B{}^2)+\frac{\pi}{8}*d_K*(D_A-d_K)*(x+2)x \quad (10)$$

$$x = \sqrt[3]{\frac{l_K * d_K}{D_A^2}} \tag{11}$$

where

K_J = Spring constant of compressed parts

$F_{CL} = F_B = F_M$ = Compressive force of preload

l_K = Combined thickness of the clamped parts

Δl_K = Change in thickness of the clamped parts

A_{Red} = Cross-sectional area of equivalent cylinder

d_K = Diameter of the bearing surface of the bolt or nut

D_A = Outer dimension of the equivalent cylinder

D_B = Diameter of the bolt hole

x = Dimensionless constant

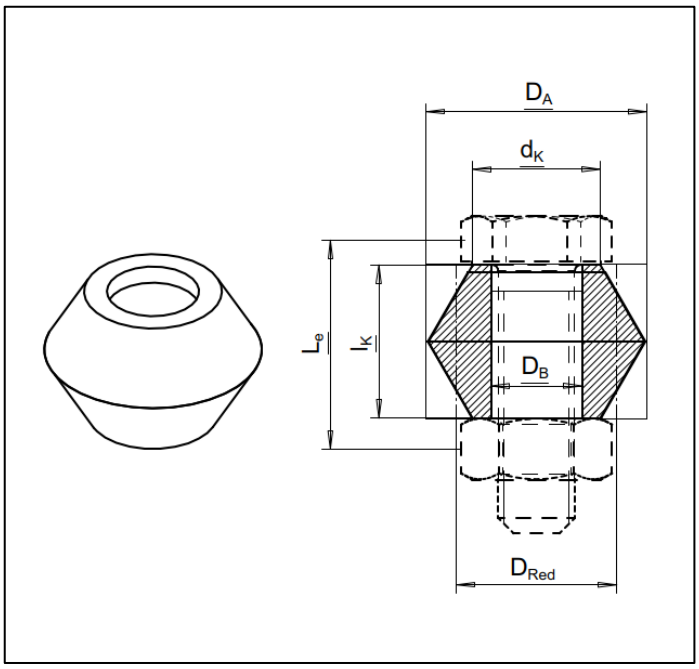

Figure 11. Equivalent cylinder representing body of compressed parts (modified from Airila et al. 2010, p. 200).

2.3.2 Joint diagrams

Joint diagrams illustrate the relative stiffnesses of the bolt and compressed parts in a bolted connection and can also visualize the effects of external loads. The ratio of relative stiffnesses which is often referred to as stiffness ratio or load factor is presented in the following equation as Φ_K. The load factor is a dimensionless constant that indicates the distribution of external loads between bolt and compressed parts, that is possibly modified by Loading Plane factor *n*, with a value between 0-1, which indicates the way load is applied to the connection such as in a directly along the bolt axis where the value of *n* is 1. When force is exerted indirectly it is better to assume a value of 0.5 (Bickford 2008, p.242).

$$\Phi_K = \frac{K_B}{K_B + K_J} \tag{12}$$

A basic form of joint diagram without the effect of external loads is seen in figure 12, where F_{PL} presents the initial preload and the slopes of spring constant lines K_B and K_J ratio of stiffnesses between bolt and compressed parts.

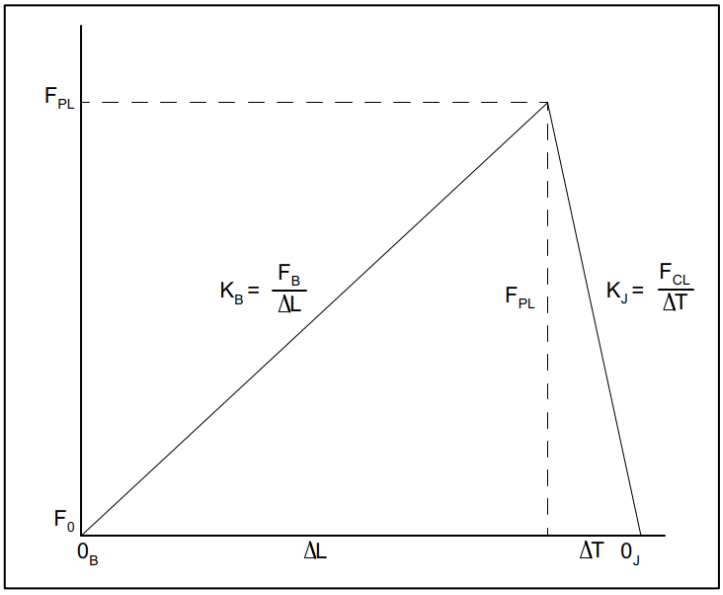

Figure 12. Joint diagram of a pretensioned bolted joint (modified from Bickford 2008, p. 113).

2.3.3 The effect of lubrication

There are three basic types of lubricants used in threaded connections, which are oil-based liquids, pastes and dry film lubricants. The oil-based lubricants are typically mineral or synthetic oils with added substances such as silicone, esters, olefins, glycols and polybutenes. Pastes have solid lubricants such as graphite or molybdenum disulfide mixed with oils or greases and dry film lubricants have the lubricating solids dispersed in binders such as epoxies or silicones. (Novak & Patel 1998, p. 48-49)

When using torque to preload bolted joint most of the used energy is dissipated in overcoming friction between different surfaces. According to Bickford (2008) roughly 50% of the total force is lost in overcoming friction between nut and the clamped parts, 40% in the friction between mating threads and only 10% of the developed into useful clamping force within the connection. He also suggests that by applying lubrication between mating surfaces not only the friction coefficient can be reduced but preload scatter as well resulting in more uniform clamping force in connections with several bolts. The reduced coefficient of friction also reduces the amount of torque needed to create clamping force, which reduces the torsional stresses during preloading and protects mating thread surfaces from wear such as galling during installation.

Lubrication can also have a positive effect on fatigue strength of a bolted connection and be beneficial if the bolt is retightened. A study by Kraemer et al. (2022) on a controlled test with different lubricants suggested that depending on the lubricant both the crack initiation and propagation times could be increased and fatigue strength in general was increased regardless of the lubricant type when compared to unlubricated bolts. Highest improvement on crack initiation time was reported on paste lubricants and highest improvement in crack propagation time with oils. Another study by Liu et al. (2022) suggested that in bolted connections that are retightened the original preload values couldn’t be reached during retightening on unlubricated test pieces. The results were contributed to surface damage between threads during initial tightening which is less pronounced with lubrication.

Lubricity can also have some mixed effects such as ease loosening of the joint which can lead to several problems such as increased chance of fretting corrosion in dynamically loaded connections where self-loosening is not prevented by other means.

2.3.4 The effect of thread pitch

Thread pitch has notable effect on many properties of a bolted connection. In addition to changing the level of available clamping force and tensile stress area it has clear effect on fatigue strength of bolts. The effect of thread pitch on fatigue strength was studied by Dragoni (1997) where he concluded that for large diameter bolts the coarse threads are superior in terms of fatigue life due to the reduced stress concentration factor. Possible positive effects linked with finer-pitch threads include lesser sensitivity to SCC suggested by Bickford (2008, p. 368), which he attributed to the nature of the thread as a discontinuity where deeper thread lowers the threshold stress required for SCC more. The effect of root radius is studied in more detail using Finite Element Analysis (FEA) in the following chapter 4. of this research.

2.3.5 General application of preload

Pretension in a bolted joint be achieved by using thread geometry and torquing the nut or the bolt or by stretching the bolt to a predetermined amount by some other means, such as specialized equipment like hydraulic tensioner or by heating the bolt and using the effect of thermal expansion and contraction. The general form which illustrates the level of available preload is shown in figure 13, which broadly follows the familiar stress-strain curve of steel materials. During initial elastic region the tension and elongation of the bolt material is roughly linear which ends at the elastic limit located near the yield strength of the material. When tightened beyond elastic limit the material stretches permanently and ability to provide reliable clamping force may be compromised, which usually leads to yield strength being considered the practical limit of available preload.

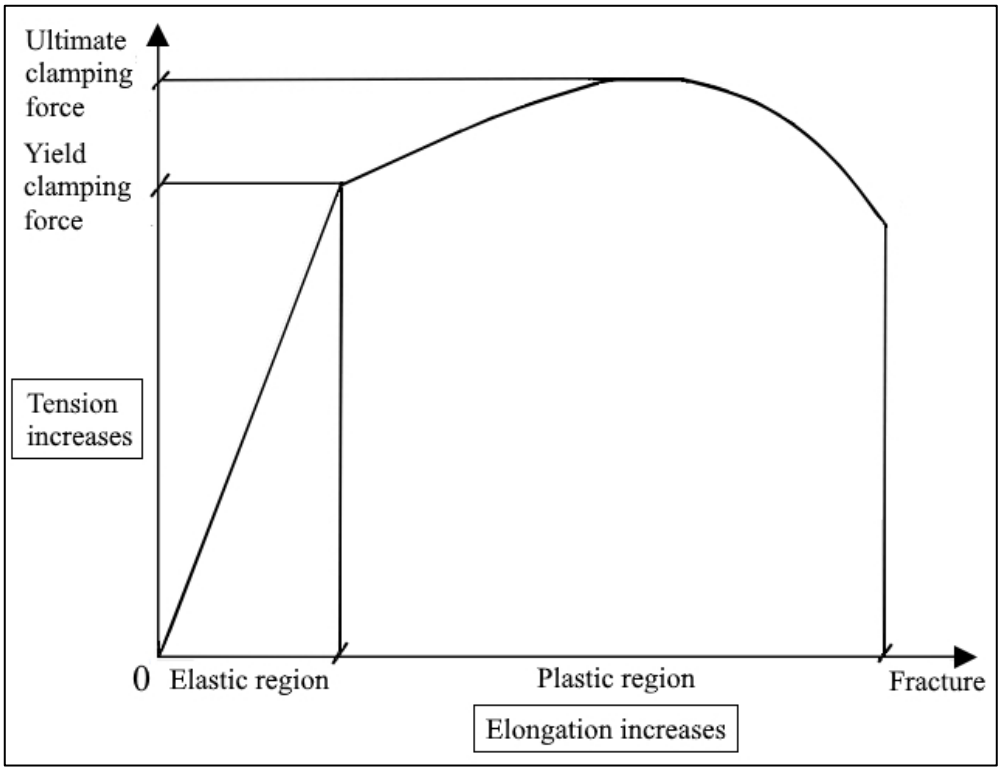

Figure 13. Available clamping force during pretensioning (modified from Oberg 2020, p. 1662).

In calculation of preload the main goal is to ensure that the connection its constituent parts can sustain the maximum load from preloading and in-service conditions and doing so retain enough clamping force to prevent separation of the parts. When the in-service conditions contain hard to define loads or load combinations such as loads from eccentricity, differential thermal expansion or dynamic forces the designs are made with sufficient factor of safety which account for any uncertainty. The final in-service conditions also usually pose certain losses to the true level of preload through embedment, relaxation or elastic interactions between parts. These losses in addition to inaccuracies of tools and assembly methods dictate the range of final in-service preload. To account for these factors there are comprehensive set of procedures in the VDI (2015) standard to guide the design process, and an adaptation of VDI procedures by Bickford (2008, p. 427-440) is presented in the next sub-chapter.

2.3.1 Preload calculation process

According to adapted VDI procedures by Bickford (2008, p. 427-440) the calculation process for preload begins by assessing the geometry of the connection and estimating approximate external force L_X. After identifying the preconditions and selecting the initial bolt size and material the calculation process aims identify the target preload either from load conditions or simply by material limits of the bolt or connected parts. When calculating from minimum requirements related to load conditions the first step is to identify the minimum required clamping force F_{Bmin}, which needs to be greater than the combined losses from joints external forces ΔF_J, relaxation ΔF_P, and minimum force requirements ΔF_{Prqd} for reliable connection that resists fatigue, fretting, slipping and, if applicable leaking. The design calculations can also be further detailed by adding effects of differential thermal expansion or creep. Conditions for the basic calculations are expressed in following equations:

$$F_{Bmin}=(\Delta F_J+\Delta F_P+\Delta F_{Prqd}) \tag{13}$$

$$\Delta F_J=(1-n*\Phi_K)*L_X \tag{14}$$

After establishing the minimum force requirements, the range between minimum and maximum forces is calculated by multiplying the minimum force with a coefficient of scatter αA, which can be approximated from assumed percentage of scatter s according to equation 16. The resulting maximum force F_{Bmax} is used to compare to the mechanical properties of the parts in the connection and size them accordingly. Finally, the target force F_B during the assembly process is the average of F_{Bmax} and F_{Bmin}.

$$F_{Bmax} = \alpha A * F_{Bmin} \tag{15}$$

$$\alpha A=\frac{1+s}{1-s} \tag{16}$$

$$F_B=\frac{F_{Bmax}+F_{Bmin}}{2} \tag{17}$$

The percentage of scatter is dependent on the assembly method and available means of controlling residual preloads. For instance, according to VDI (2015, p. 120-121) suggested values for αA range between 1.4 − 1.6 in case of tightening with torque wrench, and for elongation-based tightening with ultrasound monitoring lower values of 1.1 − 1.2 can be used.

After the parts in the connection have been selected the calculation process is concluded by analysing the properties of the parts in mechanical and fatigue strength and contact pressures. For fatigue and mechanical strength, the aim is for the bolt to satisfy the conditions expressed mathematically in the equations below, which dictate that the maximum load at endurance limit σA must be greater than cyclic loads modified by load factor, and the modified yield strength of the bolt must be greater than the maximum force from preload and load factor modified external force ΔF_B.

$$\sigma_A \geq n * \Phi_K * (L_X - L_{Xmin})/2 \tag{18}$$

$$R_{eB} * vp \geq F_{Bmax} + \Delta F_B \tag{19}$$

$$\Delta F_B = n * \Phi_K * L_X \tag{20}$$

If parts pass the final design checks the preload force is accomplished by methods and equations described in the next subchapter. The critical external force load L_{XCrit} where the parts of the connection separate and the bolt takes the entire external load is usually roughly equal to the preload force, which is the main reason high preloads are usually recommended in all scenarios. An exception to the aforementioned recommendation dynamically loaded conditions where unnecessarily high preload can only serve to increase mean stress level and shorten the fatigue life if the maximum external loads are already well below the critical level. The effect of preload in a bolted connection is illustrated in figure 14.

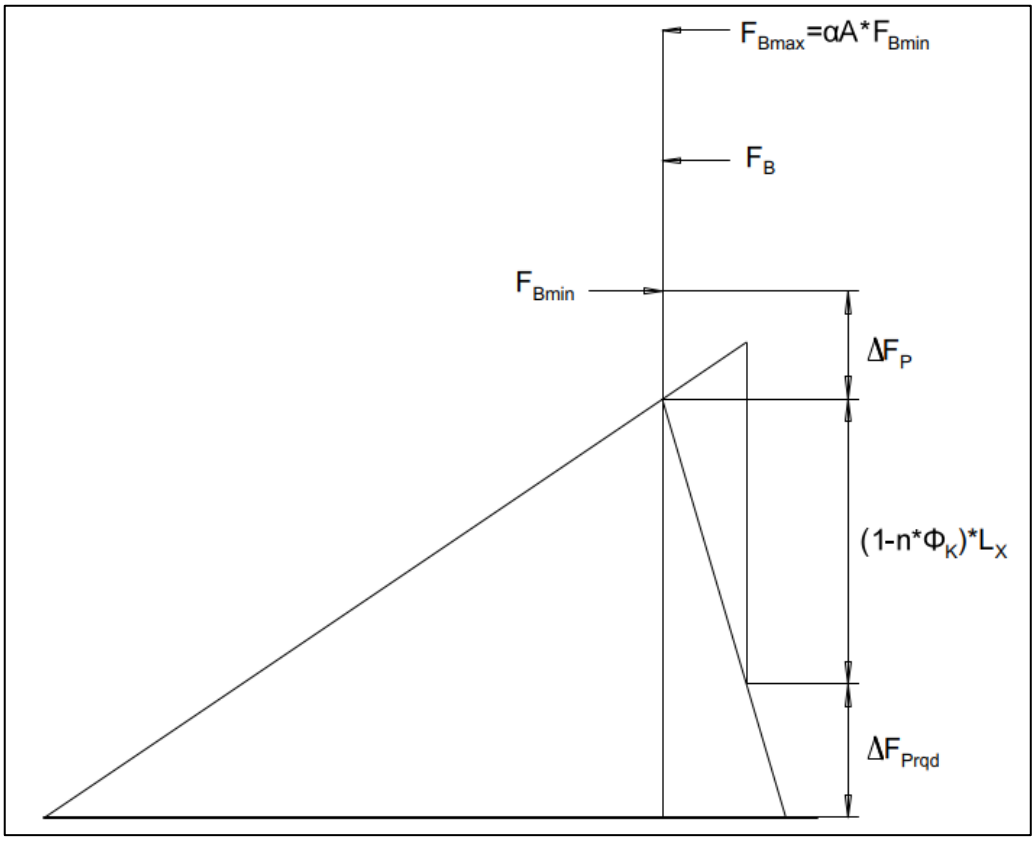

Figure 14. Combined joint diagram illustrating relations between preload and external forces (modified from Bickford 2008, p. 432).

2.3.2 Tension equations

If the conditions are sufficiently well known and connection is made using standard fasteners the calculation of preload can be done in a non-critical connection by a simple torque-tension equation.

$$T=K*d*F_B \tag{21}$$

where

T = Torque during assembly from general equation

K = Coefficient often referred to as Nut Factor with a typical value of 0.2

d = Basic major diameter of the internal thread of the bolt

F_B = Axial force obtained during assembly

In situations where increased accuracy is needed the calculations can be made using equations 22-24 that consider the effect of friction in more detail. The variables in the equations are closely linked to the pressure cone developed during tightening visualized previously in figure 11. According to Airila et al. (2010, p. 231) final accuracy of the following equations is still largely dependent on the correctness of estimated friction coefficients and the accuracy of the tightening method.

$$F_M = \frac{2*M_A}{1{,}155*\mu_G*d_2+\mu_K*D_{km}+\frac{P}{\pi}} \quad (22)$$

$$M_A = \frac{1}{2}*F_M(1{,}155*\mu_G*d_2+\mu_K*D_{km}+\frac{P}{\pi}) \quad (23)$$

$$D_{km} = \frac{d_K+D_B}{2} \quad (24)$$

where

F_M = Axial force obtained during assembly from detailed equation

M_A = Torque during assembly from detailed equation

μ_G = Frictional coefficient between mating threads

μ_K = Frictional coefficient between mating surfaces of the clamped material and the nut or bolt shank being torqued

D_{km} = The average diameter of the circle of friction

The use of thermal expansion has a long history as an option to torque as a method to obtain the high preloads on large bolts. When using thermal expansion, the bolts are initially heated

to a predetermined temperature where they stretch linearly by their thermal expansion coefficient, and then installed and tightened to a firm state by hand or a tool. During cooldown the bolts shrink and develop the necessary preload. The necessary temperature to reach a predetermined level of force can be calculated by following equations based on Hooke's Law:

$$F_B = \sigma_B * A_s \tag{25}$$

$$\sigma_B = \frac{\Delta L}{L_0} * E \tag{26}$$

$$\Delta L = \frac{R_{eB} * v_p}{E} * L_0 \tag{27}$$

$$\Delta T = \frac{\Delta L}{\alpha * L_0} \tag{28}$$

where

σ_B = Tensile stress on the bolt

L_0 = Initial length of the bolt

R_{eB} = Yield strength of the bolt

v_p = Utilization level of bolt's yield strength with typical maximum value of 0.9

ΔT = Change in temperature

α = Material specific coefficient of thermal expansion

The use of thermal expansion can offer some distinct advantages such as eliminating torsional stresses during tightening, which increases the maximum level of obtainable preload during assembly, and lot of the uncertainty regarding frictional coefficients between different surfaces. The variation in the amount of relaxation between individual bolts can also decrease as the preload build up during cooldown process more gradual and affects individual bolts in relatively uniform manner. However, the heating process is much less

convenient and may contain its own accuracy risks along with safety hazards of handling heavy heated objects, and thus the use of torque to obtain preloads is much more common.

3 Methods

This chapter details the methods used in this research. Focus is on the principles of Double Diamond methodology and the analysis of mechanics of shredder rotor. Both qualitative and quantitative methods were used in order to define the problem areas and use simulations to test design improvements.

3.1 Double Diamond process model

In the heart of the Double Diamond model is concept that the process is always either diverging or converging, where the initial step is focusing on defining and gaining insight to the problem, and second step focuses on developing solutions to the problems identified in the first step. Visualization of the flow of the Double Diamond process can be seen in figure 15 below.

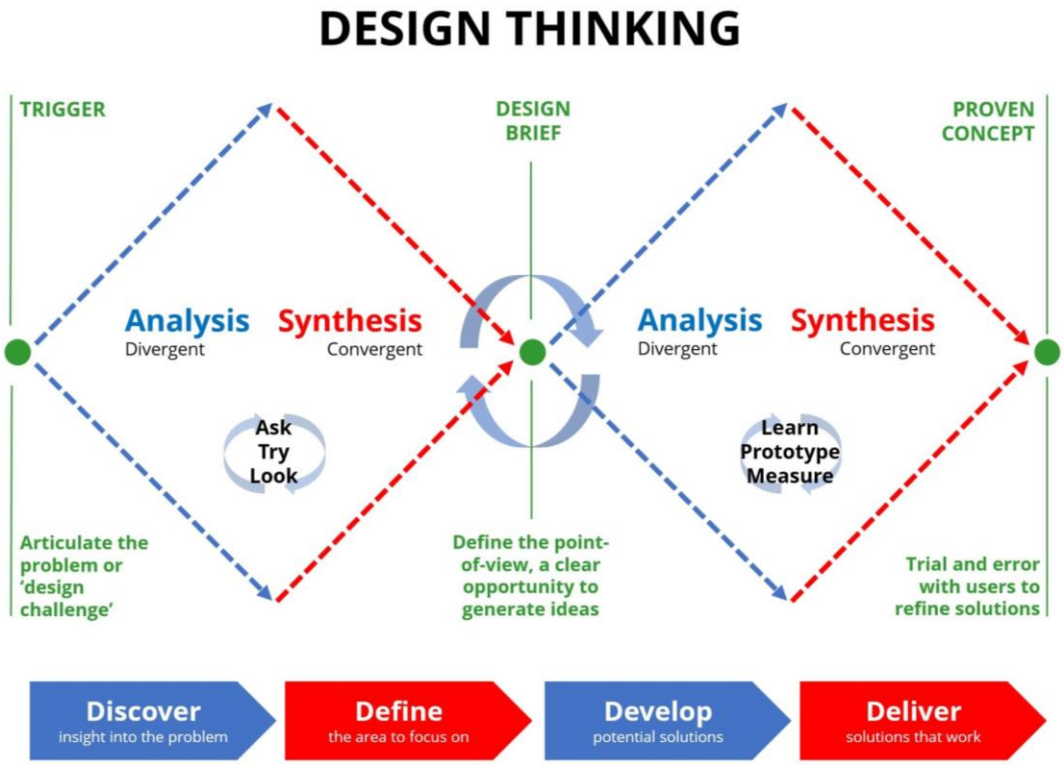

Figure 15. Double-Diamond process model (Buckley 2017).

In this research the concepts of Double Diamond are initially used to explore possibilities and find support from different sources to conclusions which point to the area of focus that will be improved during the research. Aim is to consider and narrow the list of possible reasons that contribute to failure and combine the available data from literature, user experiences, and samples to establish the most probable failure mechanic and location that can be the focus of the subsequent phase. The process of first Diamond can be seen in figure 16.

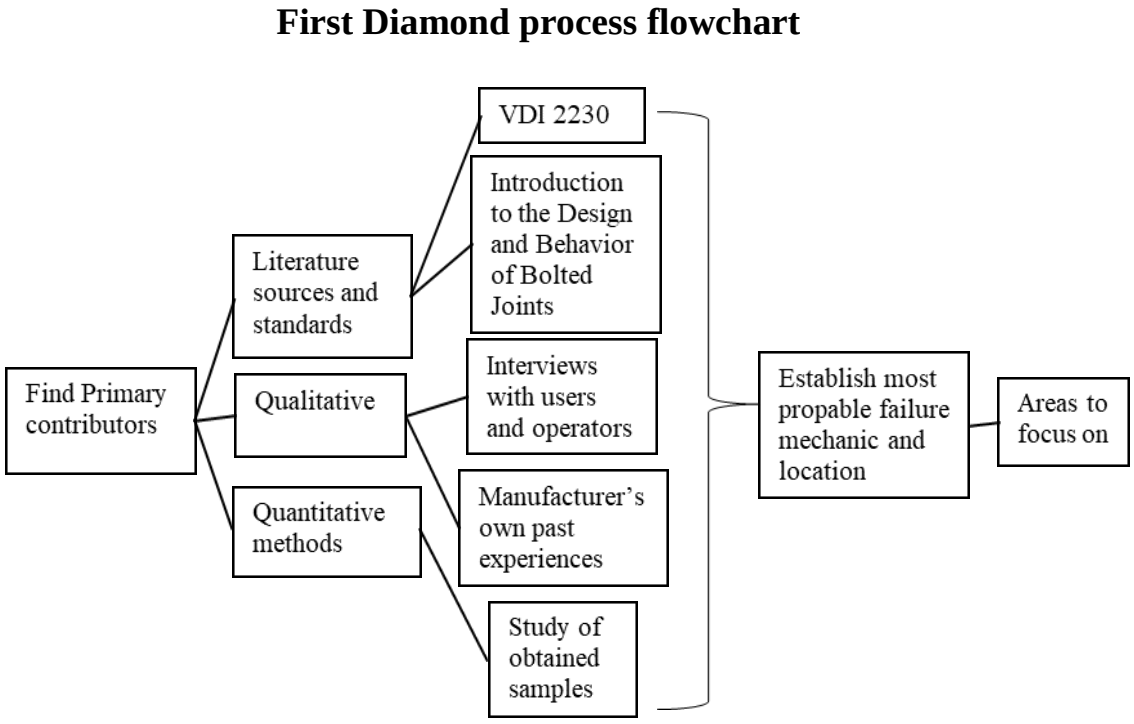

Figure 16. Process flow chart during initial Diamond.

Once the area of focus is sufficiently clear the problems are addressed by guidelines from the literature sources such as VDI 2230 (2015, p. 128) and results, if possible, validated using prototype and FEA analysis. The VDI instructions for improving reliability of a bolted connection emphasize three main factors, reducing load and stress induced to the parts and increasing their ability to withstand them. The process of second Diamond can be seen in figure 17.

Second Diamond process flowchart

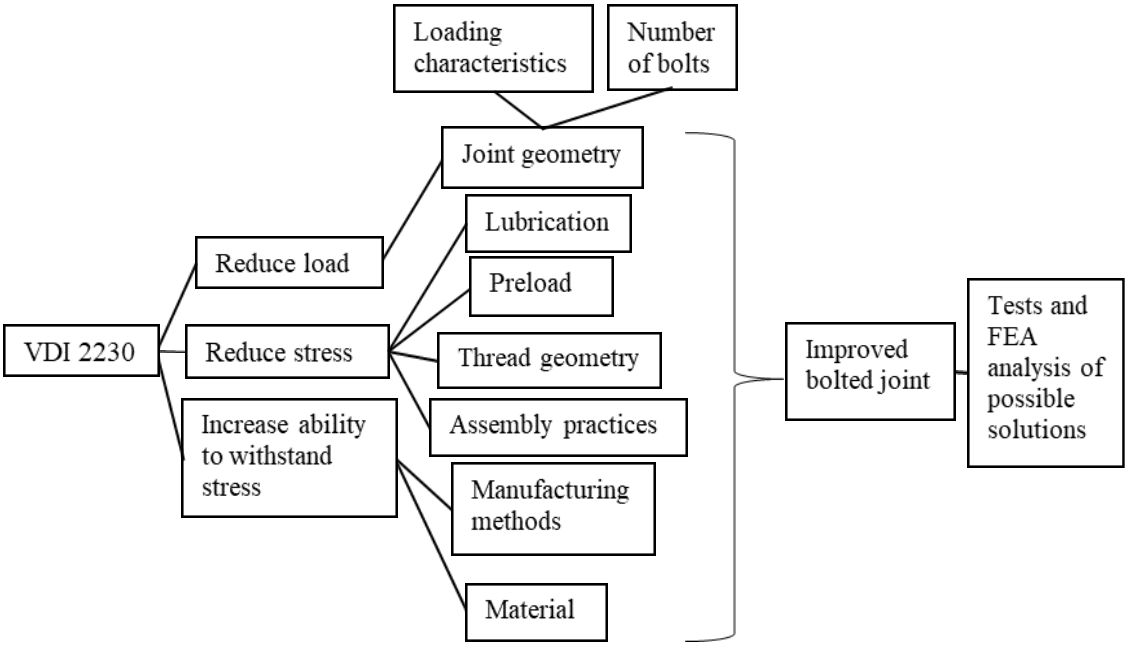

Figure 17. Process flow chart during second Diamond.

3.2 Interviews with shredder operators

Interviews with the domestic shredder operators and maintenance personnel are the main qualitative methods used in this research. Main focus was to gain insight to the possible problems the users were having with their machines and whether those problems were related to tie bolts and how. Secondary focus was to help define the main failure mechanic and location that should be addressed during this research. List of main questions presented in the interviews can be seen in table 1 and appendix 1.

3.3 Study of the samples

Study of the samples received from an operator that had a recent bolt failure was the main quantitative method used in the research in addition to simulations. The samples were

studied to see if the failure mode found in the sample would show common aspects, and if any patters could be identified from the experiences found by the operators and the main causes identified from literature.

3.3.1 Objective and method study with the samples

The object of the sample study was to establish what was the likely cause for the first bolt fracture and to see if any visible cracks, defects, or other similarities could be found from the other samples that match findings from the broken bolt. The study of the bolts was limited to visual inspection after cleanup with a wire brush and a solvent mixture.

3.4 Prototypes and Finite Element Analyses

FEA plays a significant role in helping to define possible improvement areas and assess the effectiveness of improvements. During the second diamond process the joint geometry and bolt thread were studied using Ansys 2022 R2 software. The aim of joint geometry study was to assess connection performance and the stresses in tie bolts from external load, with the possible benefits relating to different preload levels and tie bolt location and spacer design. The aim of bolt thread root geometry study was assessing the possible benefits of larger root radius. The basic material profiles used in the studies were the standard structural and low alloy 4140 steel profiles found from the Engineering Database of Ansys software. The 4140 is a steel grade from American standardization organizations such as Society of Automotive Engineers, which is equivalent to 42CrMo4. In the thread root study, the low alloy 4140 steel profile was updated with Bilinear Isotrophic Hardening property to increase accuracy by including the effect of strain hardening with tangent modulus 2125 MPa following the E/100 assumption for stress strain curve in the plastic region from recommended practice guideline of DNV GL (2020).

3.4.1 FEA of bolts within rotor geometry

An analysis of stresses in tie bolts during operation was concluded using example rotor with values relating to drive performance, masses, and dimensions as general assumptions for a

shredder of such size. The calculation of analysis loads was adapted from a model suggested by Kinnunen (2008) which can be seen in appendix 2. In his model the main thought behind establishing analysis loads is the assumption that maximum radial loads in normal operation happen when all the hammers in a single pin make a hard contact with scrap that is sufficient to temporarily nullify the balance of centrifugal forces. In such cases at the moment of hard contact the rotor is assumed to have point loads equal to the combined centrifugal forces of hammers in the opposing pin. For simplification purposes the forces from the hard contacts are assumed to happen directly below the rotor resulting in opposite forces to static mass which partly cancel each other, and the analysis therefore contains loads only in one direction.

The analysis was concluded using a 3D linear static structural study with a quarter-symmetric model and simplified geometry comprised of shaft, spacers, rotor disks, end disk and tie bolts. The interaction between different parts in the model were solved with different contacts. No-separation contact, which prevents parts from penetrating or separating from each other but allowing frictionless sliding was used to link spacers and disks to the shaft and tie bolts to the disks and spacers. A bonded contact which prevents all movement between surfaces was used between tie bolt heads and end disk to transmit preload and frictional contacts with 0.2 coefficient of friction was used between spacers and disks. Motion of the model was prevented by anchoring the shaft with remote displacement at the assumed location of the bearing which prevented motion, but allowed rotation, around the main axis. The analyses contained two steps, both with 10 sub steps, and with generally coarse mesh that was refined mainly around the surfaces of tie bolts. In the first step the initial preload to tie bolts was set and in the second step the analysis load was gradually added to the center of the rotor shaft. The analysis setup for one of the simulations with 750 kN bolt preload, modified tie bolt and spacer design, and external force acting in 45° angle to the bolts can be seen in figure 18.

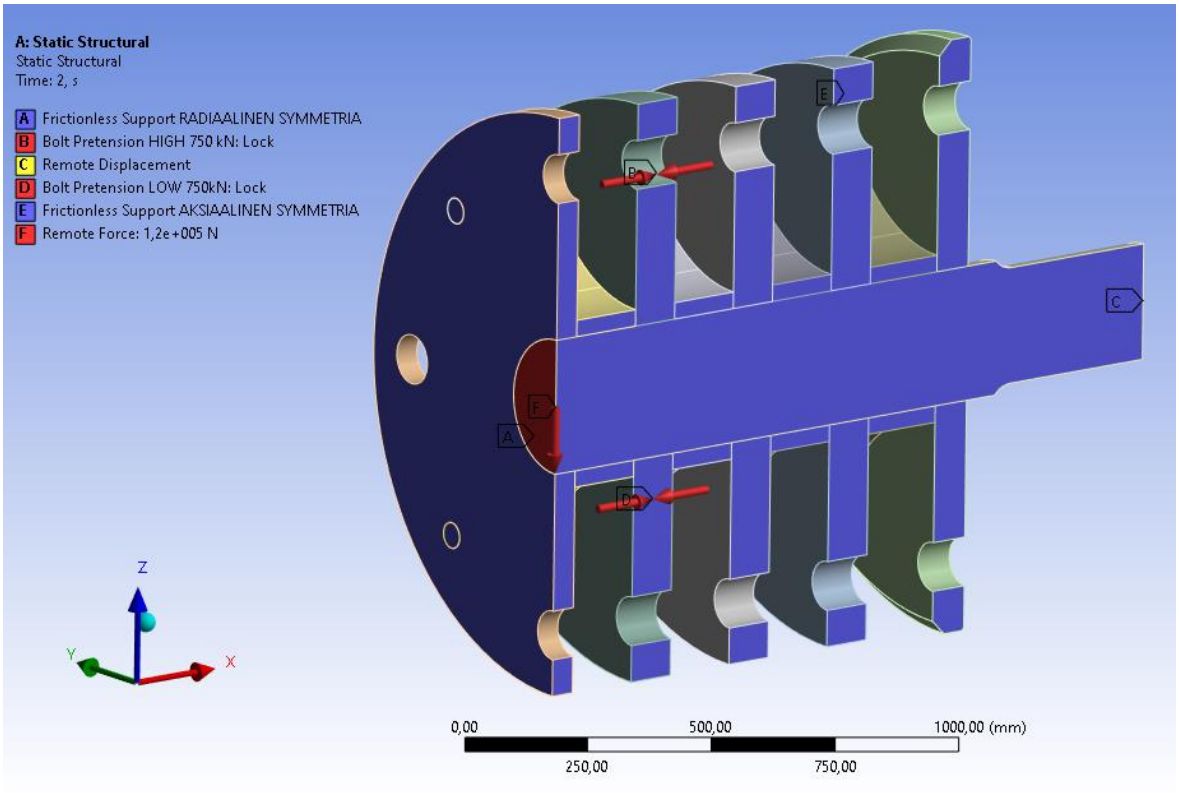

Figure 18. General analysis settings in rotor design studies.

The analyses were performed with load acting in parallel with bolts as well as in 45° angle. The bolt preloads in the simulations were 550 kN and 750 kN, which translates roughly to 60% of 8.8 and 10.9 Graded M52x5 bolts yield strength during installation by torquing. Two different tie bolt locations and spacer designs were also evaluated, one with traditional small spacers and tie bolts close to the shaft and an alternative design with tie bolts at the outer edge of the disks and modified spacer design. Both designs can be seen in figure 19 where the left configuration is the traditional and right configuration the alternative design.

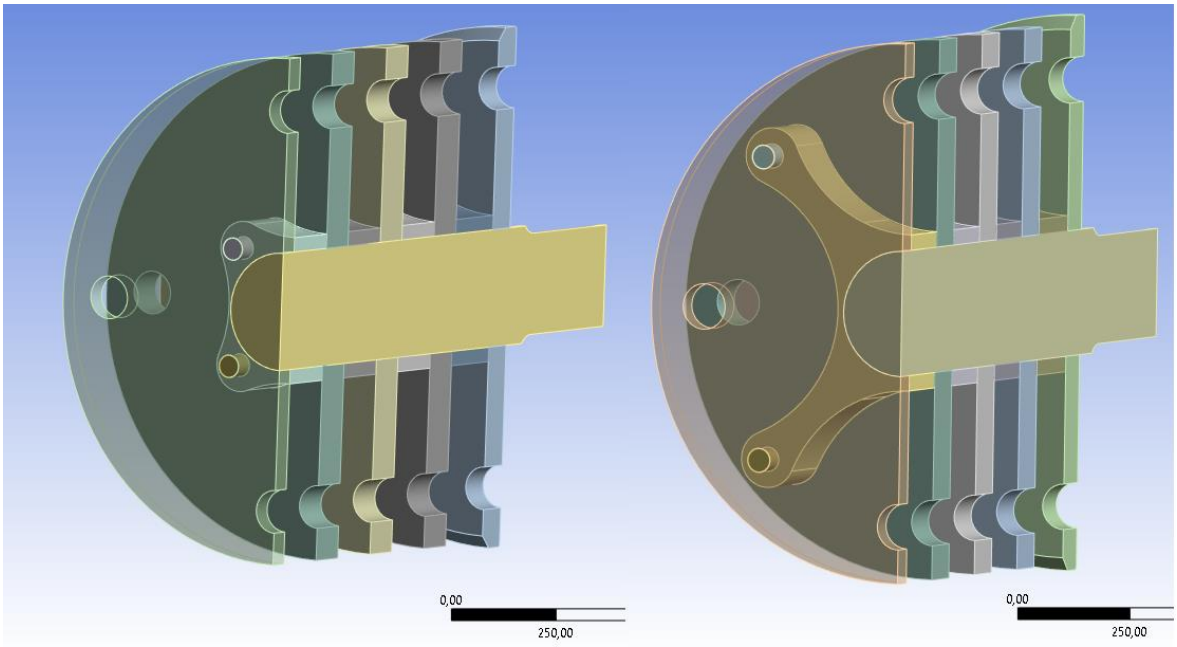

Figure 19. Analysed tie bolt and spacer designs side by side.

The objective of the rotor design analyses focused on performance of the designs in terms of rotor stiffness which was measured by directional displacement when loaded and contact between center rotor disk and adjacent spacer. The objective was also to study the effect of external load on average normal stress at the stretched tie bolt. The data could then be used to assess the effectiveness design change on joint geometry as a part of the second diamond process.

3.4.2 FEA of bolt thread geometry

As a possible improvement for reducing stress and improving tie bolt fatigue life a prototype M76x4 tie bolt head with increased root radius was created by using standard cutting tool with a larger nose radius intended for M76x6 coarse thread. The general equation for thread root radius can be seen below where *P* is equal to the thread pitch, and for the analyses the thread root radius of the prototype is assumed to be equal to the result given by the equation.

$$R_{Root}=0.144*P \tag{29}$$

The thread of the prototype bolt head was manufactured to a nominal standard tolerance of 6g to accompany 6H nut. After manufacturing the prototype, the pitch diameter of the resulting thread was measured and modelled from the measurements using Computer Aided Design (CAD) software in order to compare it against standard M76x4 thread manufactured at nominal tolerances. The comparison was done using a bilinear 2D-axisymmetric model of a tie bolt head that was loaded axially with loads equal to torquing the bolt to 60%, 70% and 80% of low alloy 4140 steel yield strength at assembly. The preload calculations were done using equations listed in chapter 2.3 assuming 0.15 coefficient of friction on all surfaces, standard nut dimensions, zero losses from relaxation or elastic interactions and 100% accuracy on torque-tension relationship, with the resulting axial force used in the analyses.

The mating surfaces of the bolt and nut threads were assigned frictional contacts with coefficient of 0.15 and surface treatment of the contacts were adjusted to touch to ensure contact with mating surfaces despite the modelled gap. The movement of the model was constrained by preventing movement of modelled bolts bottom surface and load was introduced to the bottom of the nut. The number of mating threads on the nut was assumed to be 14. The overall mesh density in the analysis was set to 1 mm quadratic mesh with 0.2 mm edge refinement at mating threads. To increase accuracy further the software was tasked to use adaptive mesh refinement and convergence with maximum allowed change set at 5%, which results in further mesh refinement rounds if results between rounds differ by more than allowed. The analysis settings and 2D-axisymmetric model used in thread root radius studies can be seen in figure 20.

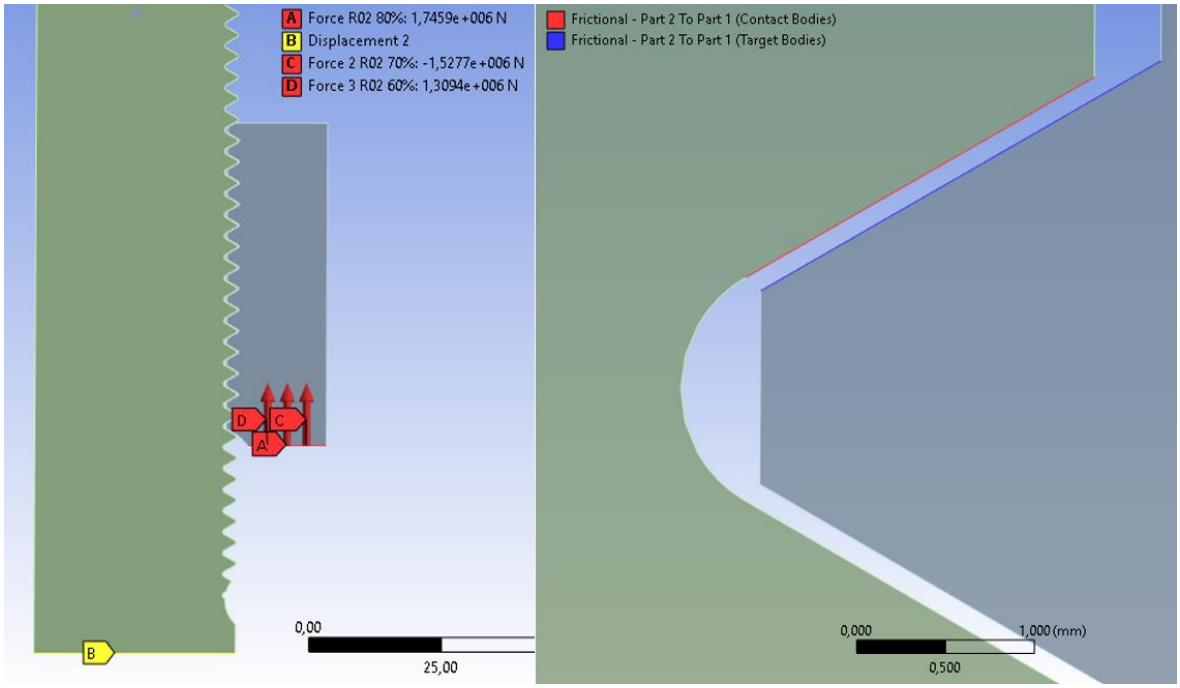

Figure 20. Analysis settings for tie bolt thread root studies.

The objective of the analysis was to assess the level reduction in principal and mean stresses, shear stresses and total strains at the thread root using different loads and to establish preliminary estimate of the effect of larger root radius to results and as such focused purely on the bolt thread. The analyzed load situation was not intended to represent specific in-service conditions but instead to focus on assessing the effect of a geometry change in a simple load scenario, with the assumption that the resulting changes could be considered as a comparable generalized result.

4 Results

This chapter details the results of interviews and the analyses of obtained tie bolts samples studied in this research. The results from the FEA and material change considerations are summarised at the end of this chapter.

4.1 User experiences of shredder operators

Operators of Finnish shredding facilities were asked to share their experiences to the research. The amount of experience that interviewees had was mixed and as a generalized time window they were asked to consider a period of last five years. The questions and answers can be seen in tables 1 and 2.

Table 1. The questions presented to shredder operators.

1.	Have you experienced any problems with the rotor's tie bolts, such as the bolts breaking unexpectedly?
2.	If you've experienced tie bolts breaking, can you identify the most common place where the breaks or failure happen?
3.	Can you recall how frequent these problems are?
4.	Can you identify any other patterns to the tie bolt failures you've experienced?
5.	In case of tie bolt breaking what is the maintenance protocol or repair procedure you follow?
6.	Do you have an opinion on what is the most likely cause for a tie bolt breaking?

Table 2. Main answers from interviews with shredder operators.

Operator interviews						
ID	**Question number**					
	1	**2**	**3**	**4**	**5**	**6**
1	Yes	Stretch	Unknown, issue ignored. Bolts are not changed.	Nothing specific.	None. Rotor disks contained by secondary fastening method. Imbalance dealed case by case with manual adjustments of hammers.	General wear and loss of preload due to stretch.
2	Yes	Break at thread	3 failures in 5 years.	In recent years more breaks have occurred.	Switch to reserve rotor and replace all bolts if rotor is undamaged.	
3	Yes	Break at thread	1 failure in 5 years.	Nothing specific.	Switch to reserve rotor and replace all bolts if rotor is undamaged.	
4	Yes	Stretch	3 failures in 5 years.	New bolts stretch and lose preload within two years.	Switch to reserve rotor and replace all bolts if rotor is undamaged. Generally avoid bolt failures by preemptive bolt replacement.	Outside influence of unshreddables most likely cause for breaks.
5	Yes	Break at thread	2 failures in 5 years.	Nothing specific.	Repair broken bolt in place if possible.	Outside influence of unshreddables most likely cause for breaks.
6	No		No experience in failures specifically with tie bolts.		Tie bolts changed only when the entire rotor is replaced.	

4.1.1 Insights from the operator interviews

The thread is reported by several interviewed persons as the most likely cause of general failure, and many also felt that outside influence of unshreddables are the primary cause of breaks. Generally oversized or wedge-like pieces of scrap were reported as typical problematic pieces that could result in large breaks involving several parts of a shredder. The maintenance protocols generally followed a switch to a reserve rotor especially if the shredding facility was equipped with crane to ease the process. Problematic issues with maintenance after a bolt failure were usually linked with limited access to the bolts, which had prompted some maintenance crews to improve their capability of repairs without removing the rotor from the shredder, or the rotors were equipped with secondary fastening method which enabled the use of a rotor with broken bolts albeit at the expense of increased imbalance.

4.2 Study of bolt samples

During the research a sample batch of tie bolt heads was obtained from an operator with a recent bolt failure in their disk rotor with six tie bolts. The samples were the threaded portions of the tie bolts that were cut from each bolt, which were changed along with the broken one as a normal precautionary maintenance protocol. The bolt heads were in randomized order and couldn’t be linked to one another since they were not marked during dismantling, and they were received as a mixed batch. Also, during dismantling some of the bolt heads were damaged by a cutting torch, which led to omitting of two of the samples and affected the entirety of inspection on three others.

4.2.1 Insights from the sample studies

The initial interest of the sample studies was the broken sample. In study of the fracture surface the broken bolt showed signs of propagating fatigue cracks in two separate locations with the main fatigue crack initiated in the first fully formed thread. The fatigue fracture surface marks seem to indicate high nominal tension stress and severe stress concentration. The fracture surface of the broken bolt sample can be seen in figures 21 and 22. In figure 21 the beach marks where the fracture surface has gradually smoothed as the crack has propagated is clearly visible and in figure 22 the ratchet marks that indicate multiple initial crack origins growing and linking up are also visible which along with the beach lines points to the origin of the crack. (ASM International 1992, p.216-217).

Figure 21. Broken bolt showing signs of propagating fatigue cracks in two separate locations.

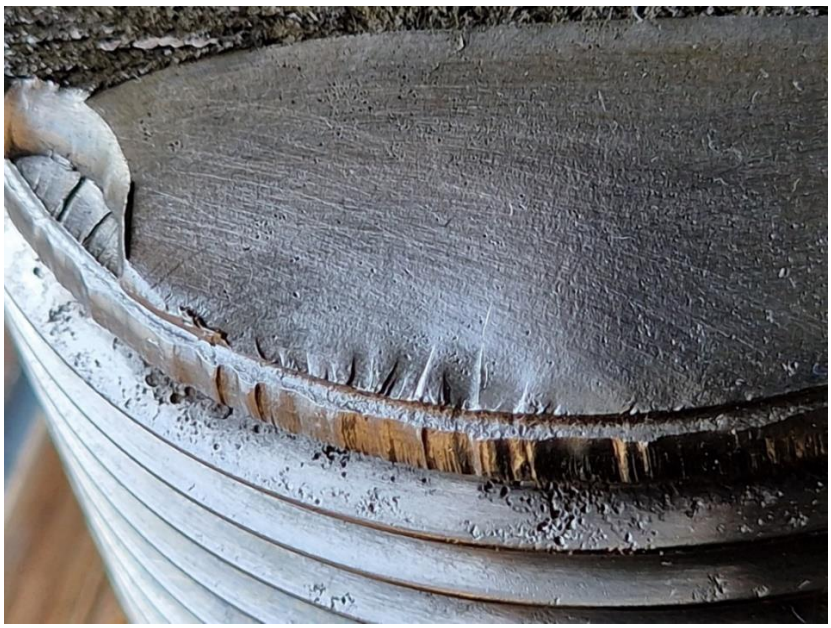

Figure 22. Main fatigue crack at the first fully formed thread with visible ratchet marks.

In the area of the thread there were also signs of corrosion. Similar signs of corrosion were also found in one of the undamaged bolt heads, with the rest of the samples showing only normal wear, which in this case is considered any surface without clearly visible pits, cracks, fractures, or erosion. Pictures of the corrosion damage found from the broken bolt and bolt head number six are shown in figures 23 and 24. The final list of the observations found from the bolts can be seen in table 3.

Figure 23. Corrosion in the threads of the broken bolt.

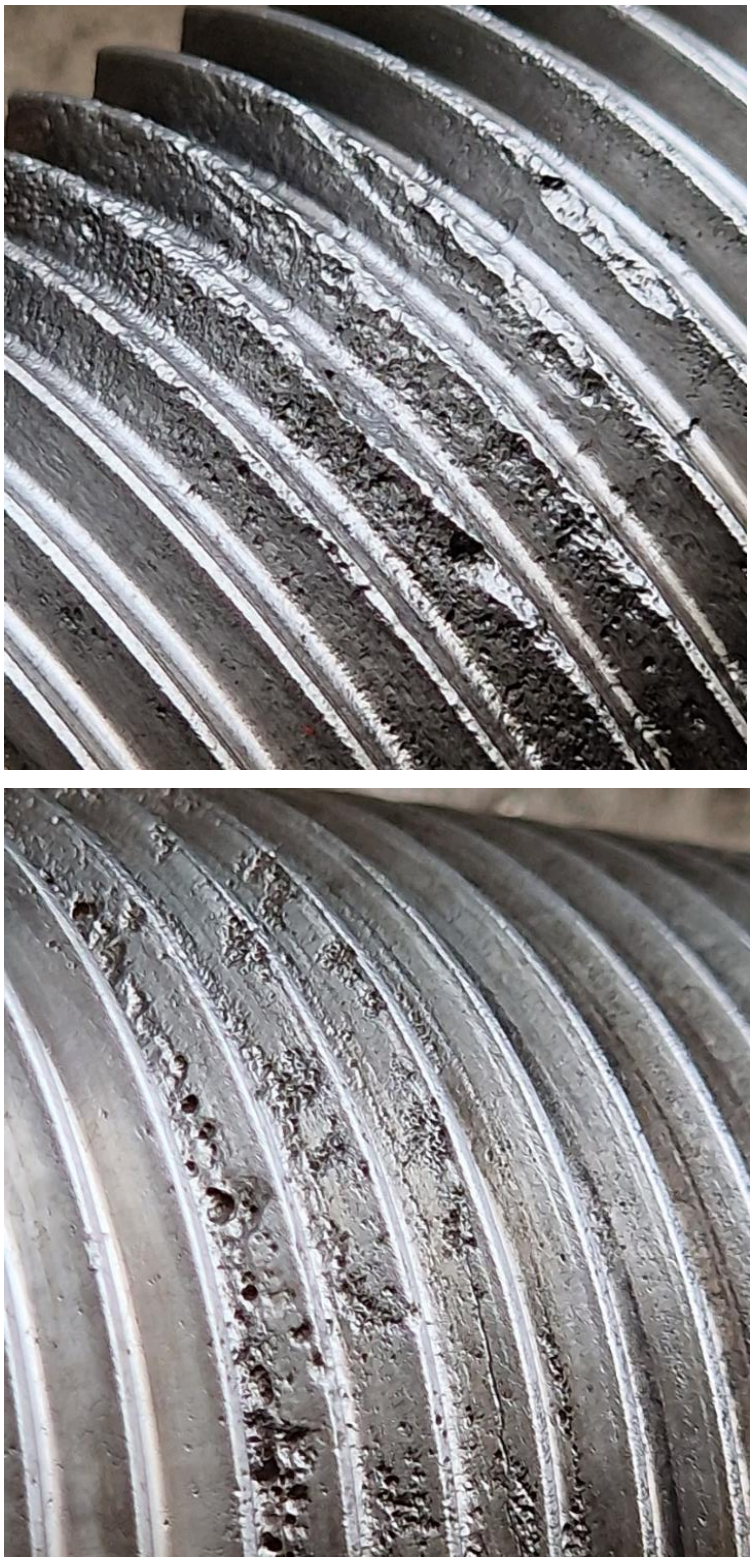

Figure 24. Corrosion in threads of one of the unbroken bolt heads.

Table 3. List of observations from bolt samples studied.

Broken bolt samples		
ID.	Condition	Notes
1	Broken	Signs of fatigue and corrosion
2	Undamaged	Normal wear
3	Undamaged	Normal wear
4	Undamaged	Normal wear
5	Undamaged	Normal wear
6	Undamaged	Signs of corrosion
7	Undamaged	Normal wear
8	Partly burned	Normal wear in unburned locations
9	Partly burned	Normal wear in unburned locations
10	Partly burned	Normal wear in unburned locations
11	Heavily burned	Not included
12	Heavily burned	Not included

4.3 FEA of rotor design

The combined results from the of the rotor geometry analyses can be seen in table 4. Listed stresses are average normal stresses at the tie bolts located in the side of tension and magnitude of external load represents results of contact studies. The contact studies aimed to assess how the connection performs under external load and fulfils the requirement of keeping clamped parts in compression throughout analysis, or at which step the gradual increase to analysis load broke the uniform contact between center disk and spacer. The result of contact study of alternative design externally loaded parallel to tie bolt can be seen in figure 25, where time of 1.8 seconds is the last point where uniform contact remains with 80 % of the total external load being applied. Overall, the simulation results suggest that increasing the size of spacers and changing the location of tie bolts further away from the shaft has notably positive effect on overall stiffness of the rotor as the displacement are almost halved and the change in stiffness also affects positively to the level of change in tie bolts stresses when external load is applied.

Table 4. Results from rotor design FEA analysis

Rotor FEA test results						
Traditional design						
	Force at 45°			Force in parallel		
ID	Value	Value	Unit	Value	Value	Unit
Preload	550,00	750,00	kN	550,00	750,00	kN
Rotor displacement	1,48	1,47	mm	1,47	1,45	mm
Bolt preload stress	260,10	354,69	MPa	259,81	354,29	MPa
Stress after external load	277,41	371,91	MPa	285,13	378,57	MPa
Stress change	17,31	17,22	MPa	25,32	24,28	MPa
Magnitude of external load where full contact remains	70,00	100,00	%	50,00	70,00	%
Alternative design						
	Force at 45°			Force in parallel		
ID	Value	Value	Unit	Value	Value	Unit
Preload	550,00	750,00	kN	550,00	750,00	kN
Rotor displacement	0,79	0,78	mm	0,80	0,79	mm
Bolt preload stress	260,04	354,61	MPa	259,74	354,19	MPa
Stress after external load	267,74	362,31	MPa	270,80	365,28	MPa
Stress change	7,70	7,70	MPa	11,06	11,09	MPa
Magnitude of external load where full contact remains	100,00	100,00	%	80,00	100,00	%

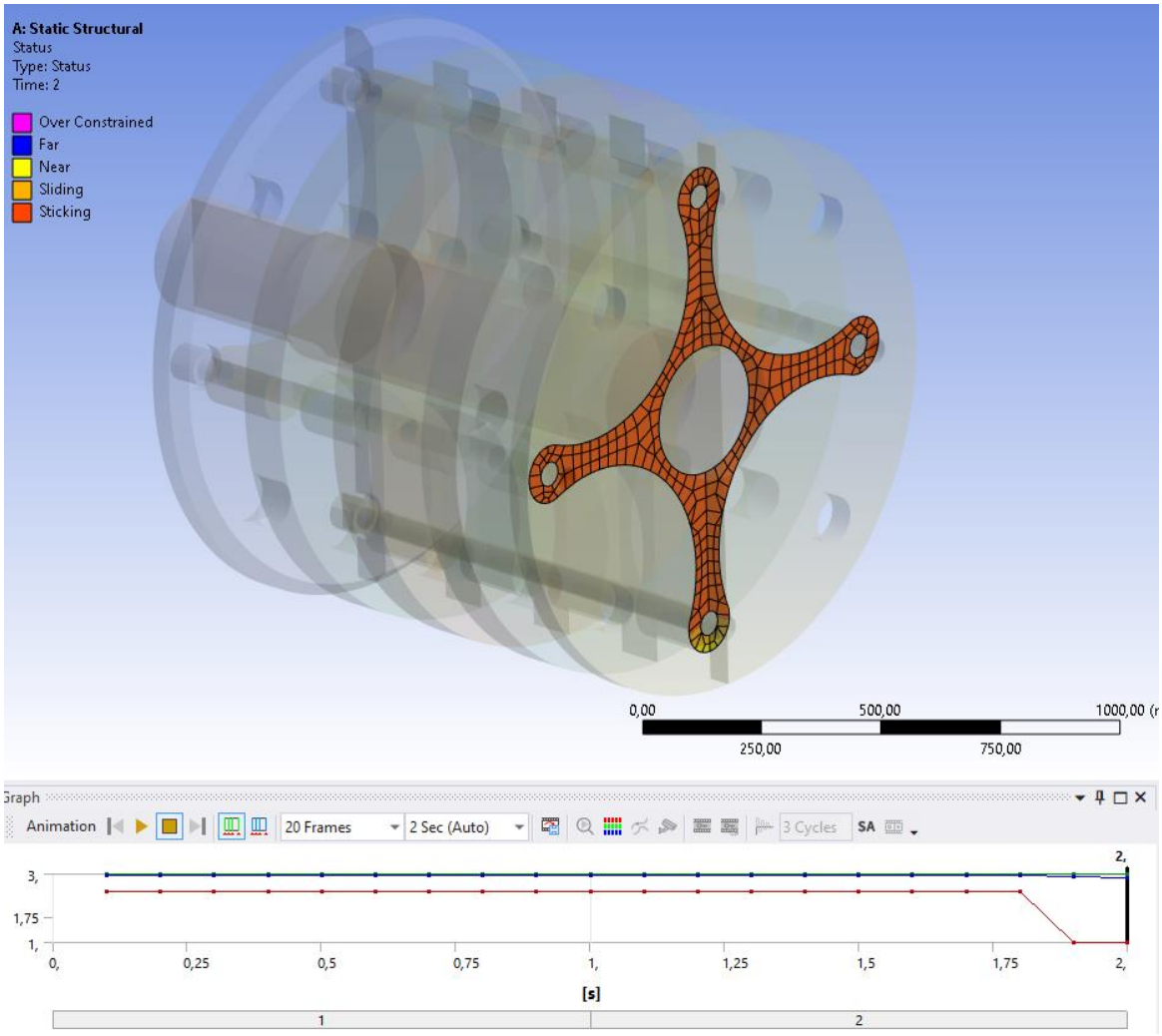

Figure 25. Results of contact study with alternative design preloaded with force of 550 kN and subjected to external force acting in parallel to tie bolt.

4.4 FEA of thread root geometry

The results from the of the thread root geometry analyses can be seen in table 5. Results followed normal pattern where the highest stresses and strains were at the root of the first engaged thread and therefore the results were only gathered from there. As the stresses locally pass the materials yield strength the studied stresses are the principal stresses and the mean stress which is the average of the sum of maximum and minimum principal stresses. The accepted principal and shear stress results listed in figure are the rounded average value

between highest and two adjacent nodes. As the total strain values were very small the listed values are the highest nodal values rounded up to four decimal places.

Table 5. Results from FEA of M76x4 thread with different root radii.

Thread root analysis results							
80% load	Root radius (mm)	Bolt force (N)	Max Principal (MPa)	Min Principal (MPa)	Mean stress (MPa)	Total Strain (mm/mm)	Max Shear (MPa)
	0,576	1,7459E+06	1075	390	732,5	0,0167	431
	0,864	1,7459E+06	1000	322	661	0,0125	417
	Resulting change [%]		-7 %	-17 %	-10 %	-25 %	-3 %
70% load	Root radius (mm)	Bolt force (N)	Max Principal (MPa)	Min Principal (MPa)	Mean stress (MPa)	Total Strain (mm/mm)	Max Shear (MPa)
	0,576	1,5277E+06	1034	363	698,5	0,0138	389
	0,864	1,5277E+06	960	290	625	0,0105	385
	Resulting change [%]		-7 %	-20 %	-11 %	-24 %	-1 %
60% load	Root radius (mm)	Bolt force (N)	Max Principal (MPa)	Min Principal (MPa)	Mean stress (MPa)	Total Strain (mm/mm)	Max Shear (MPa)
	0,576	1,3094E+06	970	291	630,5	0,0101	384
	0,864	1,3094E+06	907	246	576,5	0,0083	381
	Resulting change [%]		-6 %	-15 %	-9 %	-18 %	-1 %

The results showed consistency over different load levels and suggest that larger root radius has a positive effect by lowering overall stress levels and reducing total strain while only having small effect on the maximum shear stresses.

4.5 Tie bolt materials

Expression from the past experiences in general indicate that the material choice has not exhibited clear indications of a wrong selection. There is a long history of making the bolts from steel such as 42CrMo4 in Q&T condition throughout the industry, but as a part of the second diamond process a comparison of few different materials is conducted, with 42CrMo4 being considered the baseline material against three other readily available materials.

Basic requirements for the material are to be available in round bar sizes of up to 80 mm and the candidates are compared by their mechanical properties such as strength and hardness, weldability, corrosion resistance and notable options, benefits and risks with respect to the intended use. The aim is to identify potential opportunities to increase the tie bolt's ability to withstand stress through material change as suggested by VDI instructions. Although none of the materials is specifically corrosion resistant the possibly beneficial alloys are listed as benefits as corrosion was found on some of the studied samples. List of observations from material comparisons is shown in table 6. The material data used in this comparison is gathered from online resources of Ovako (nd.) and SSAB (nd.)

Table 6**.** List of observations from bolt material comparisons.

	42CrMo4	**4CrMn16-4**	**34CrNiMo6**	**Toolox 44**
Yield Strength, Rel [MPa]	650	700,00	800,00	1300,00
Tensile Strength, Rm [MPa]	1000,00	950,00	1100,00	1450,00
Hardness [BR]	300,00	290,00	330,00	440,00
Fracture toughness (Rel/Rm)	0,65	0,74	0,73	0,90
Weldability	Limited.	Good.	Limited.	Limited.
Corrosion resistance	Possibly beneficial Molybdenum alloying	Highest chromium content.	Possibly beneficial Nickel and Molybdenum alloying.	Possibly beneficial Nickel and Molybdenum alloying.
Notable benefits or risks	Good combination of strength and ductility. Variant option available to increase strength.	Slightly higher yield strength than standard 42CrMo4. Weldable. Good impact strength at low temperatures.	Good all-around properties including high tensile and impact strength while maintaining ductility.	Highest strength, hardness, and fatigue limit. May lead to problems with SCC and raise possibility of brittle fracture.
Approximate cost	Cost effective baseline option.	Slightly higher cost than baseline.	Higher than baseline.	Higher than baseline.

Most interesting choices from the compared materials are 34CrNiMo6 and Toolox 44, with both having higher strengths subsequently fatigue properties and alloying content which may increase resistance to atmospheric corrosion. Particularly the highest nickel content of 34CrNiMo6 is linked to many positive effects including impact strength and low temperature performance in comparison to 42CrMo4, which otherwise offers very similar in all-around performance that can be theoretically tailored to many uses by using its different variants, of which the most interesting is the variant 6115 that is available at strength grade 10.9 for up

to 60 mm diameter, which is sufficient for smaller rotors. Toolox 44 offers the highest improvement in strength, hardness and related properties such as fatigue limit, but with lowest fracture toughness in plastic area, which can present risks in conditions with high mean stress and impacts. It along with 34CrNiMo6 also increases the tie bolts material costs. However, as the tie bolts represent only a small portion of total material and manufacturing costs relating to shredder rotor, the impact of approximate cost can be considered minute. 4CrMn16-4 offers similar properties to 42CrMo4, but other than weldability doesn't offer any clearly distinctive features. It has the highest chromium alloying content, but at a level where its corrosion resistance properties are questionable. It also lacks molybdenum which improves properties of many alloys even at very low amounts.

4.6 Analysis of the FEA results and collected data

The reliability of simulations and how they represent real life situations can always be questioned as they inevitably contain simplifications and assumptions. It is also possible that available knowledge is incomplete to accurately represent the problem for the simulation software. During this research the focus of the simulations was on overall rotor design and how it affects the context where the tie bolt is intended to perform its relatively simple task of compressing parts of the rotor together.

Simplification where rotor is only experiencing external forces in one direction is likely rare and more often the spikes of opposing centrifugal force are on the opposing side of the anvil which is located at the mouth of shredder. It is also likely rare that all of the hammers experience hard contacts at the same time, but for analysis purposes the likely higher one directional load offers margin of safety against uncertainties and simplifies the interpretation of results. In addition to risks related to initial conditions FEA analyses also contain risk related to mesh density and artificially high results. Of the results obtained during this research only the strain values of thread study are likely to contain notable error relating to mesh density as the values were very small. The rotor design studies only concerned average stresses at tie bolts which agree with simple analytical results well. Similar process of evaluating the loaded deformations of the isolated shaft in 3D study and elongation of bolt in 2D study against analytical results showed good similarity which confirms that the basic boundary conditions reflect reality well.

5 Discussion

Improvement of single component in a system is always challenging as the factors that may have impact on the results can originate from issues seemingly not related to the component itself. Problematic areas experienced during this research stem from the fact that while the focus areas identified during the initial diamond showed general consistency in pointing towards the thread and fatigue resistance, the absence of detailed records, previous research or a large sample pool induced some reliance to information gathered from interviews, which can lead to data being qualitatively skewed and contain some bias from personal opinions. Other concerning issue was the lack of concrete measurements of in-service preload levels which has a strong influence on the overall performance of dynamically loaded connections.

The improvements suggested and analysed in this research are likely to improve the overall performance of tie bolts, but only if the proper preload can be attained during installation and maintained at a reasonable level during the entire service life of a rotor. In normal service conditions the tie bolts should experience relatively small changes in stress level due to radial external forces providing that the preload level is sufficient, but the overall scatter of tightening methods, dynamic conditions, shocks, as well as lack of control may lead to changes in preload that is not easy to predict or consider during design. Slip and loss of compression can induce cascading effects resulting in greatly diminished preload, which may be the reason for failures by stretching when pretension is no longer protecting the tie bolts against sudden surges of external loads. In the long run aforementioned factors and the lack retightening to restore pretension may be one of the main issues relating to failures. In addition to the mechanical aspects one of the notable improvements of rotor geometry changes, where tie bolts are located on the outer edge of the rotor and spacers are larger, are the better maintenance options as the tie bolts can be replaced without removing any of the bearings that support the weight of the rotor. This a very concrete difficulty and may be the main reason why shredding facilities without service cranes may simply opt to accept the breaks and try to manage with the less stiff rotor or attempt field repairs.

While the research focused primarily on fatigue it is not the only common reasons for failures. Outside influence in the form of unshreddables can be responsible for catastrophic multipart failures and their presence and effect is one of the issues that is very difficult to

completely eliminate with design choices only relating to the shredder. Other factors of note related to outside influence that may contribute to failures are the large fluctuations in surface temperature that the rotor can experience during Nordic winter times. The rotor temperature at startup may be well below sub-zero and once shredding of material begins the heat from friction starts to heat the rotor. It is possible that somewhere during the initial stages of working shift before the temperature becomes steady the rotor disks and the tie bolts experience differential thermal expansion, which may fluctuate the level of stresses in the tie bolts as well as the amount of compression they contribute to the rotor. In both cases the skills of the operators in identifying potentially risky materials and temperature conditions are invaluable in ensuring that the rotor can be used as closely as possible to the normal operating conditions.

6 Conclusions and summary

The main research question at the start of this research was to establish the primary reason and mechanic of tie bolt failures. The information gathered initially pointed to fatigue as one of the likely reasons for failure, which is a generally shared sentiment on numerous literature sources. Fatigue failures in metal are generally due to alternating stresses which exceed materials fatigue limit, which may be affected by several factors such as presence of stress raisers and corrosion. The presence of corrosion probably played a significant role in the failure of the bolt in the sample batch, and its presence should be observed closely in case of future breaks.

The secondary research question was that what is the optimal pretension for tie bolts, and a simple and completely exhaustive answer to that question can't be given as the factors that affect the end result are not easily identified and controlled in normal procedures. Optimal preload for tie bolts depends on several factors which have to be considered case-by-case, but in general higher preloads and material strength properties can be beneficial to both the tie bolt as well as the rotor, but care should be taken when determining initial preload level and aim for realistic estimation of the scatter with a factor of safety considering both negative and positive scatters.

The suggested improvements of this research aim to reducing load and stress induced to the parts by preliminary design changes to the rotor and thread root geometry and increasing their ability to withstand them by choosing a suitable material with mechanical abilities more suitable for harsher conditions. Updated rotor design also improves accessibility during maintenance operations. In terms of material choices there is no reason not to use a high strength material such as 34CrNiMo6, and especially when using higher strength materials any use of methods that reduce stress concentrations such as the modified thread root will be beneficial. The preliminary results from FEA conducted during this research suggested that changes to thread and rotor design enhance rotor stiffness and lower the stresses in the tie bolts. The results also suggest that in the traditional rotor design the contact between disks and spacers are more likely to be compromised by high radial loads.

The use of detailed manufacturing records and more accurate control of pretensioning should be considered in the future. Further studies should be conducted to ensure more detailed data

regarding the breaks will be available to determine the effect of factors such as corrosion in more detail. They are also beneficial in assessing the effect of suggested improvements and ensuring the right factors are being targeted by the developments identified with the Double Diamond model.

References

Airila, Ekman, Hautala, Kivioja, Kleimola, Martikka, Miettinen, Niemi, Ranta, Rinkinen,

Salonen, Verho, Vilenius, Välimaa. 2010. Koneenosien suunnittelu. WSOYpro Oy, Helsinki. 796 p.

American Society of Mechanical Engineers (ASME). 1994. The Newell Shredder. [web document]. [Referred: 16.4.2023]. Available: https://www.asme.org/wwwasmeorg/media/resourcefiles/aboutasme/who%20we%20are/engineering%20history/landmarks/179-newell-shredder-1969.pdf

ASM International. 1992. ASM Handbook, Volume 12, Fractography. ASM International, Russell Township, OH. United States. 857 p.

ASM International. 1996. ASM Handbook, Volume 19, Fatigue and Fracture. ASM International, Russell Township, OH. United States. 2592 p.

Bickford, J.H. 2008. Introduction to the Design and Behavior of Bolted Joints. 4th Edition. Non-Gasketed Joints. CRC Press. Boca Raton, Fl. United States. 515 p.

Buckley, L. 2017. Double-Diamond design thinking. [web page]. [Referred: 16.4.2023] Available: https://acumen.sg/double-diamond-design-thinking/

Dragoni, E. 1997. Effect of thread pitch on the fatigue strength of steel bolts. Proceedings of the Institution of Mechanical Engineers. Part C, Journal of mechanical engineering science. [Online] 211 (8), Pp. 591–600.

DNV GL 2020. DNVGL-RP-C208. Determination of structural capacity by non-linear finite element analysis methods. DNVGL, Høvik, Norway. 149 p.

Hyvönen, I. 2021. Fatigue Strength of a bolt under pulsating compressive stress. Master's thesis in LUT University. Lappeenranta, Finland.

Kinnunen, M. 2008. Roottorin laskentaa. RecTec Engineering Oy internal reports. Unpublished.

Kraemer, F. Stähler, M., Klein, M., Oechsner, M. 2022. Influence of Lubrication Systems on the Fatigue Strength of Bolted Joints. Applied sciences. [Online] 12 (6), 2778, Pp. 1-19.

Liu, Z., Yan, X., Zheng, M., Wang, Y., Chen, W., Li, Y. 2022. The effect of tightening again on bolt loosening under transverse load: Experimental and finite element analysis. Structures. [Online], 44, Pp. 1303–1311.

Novak, G.J. & Patel, T. 1998. 'Threaded Lubricants', in Bickford, J.H. (ed.) 1998. Handbook of Bolts and Bolted Joints. CRC Press. Boca Raton, Fl. United States. p. 43-54

Oberg, E. Jones, F.D., Holbrook, L. H., Ryffel, H. H., McCauley, C. J. 2020. Machinery's Handbook. 31st edition. South Norwalk, Industrial Press. 2978 p.

Ovako Metals Oy Ab nd. Nuorrutusteräkset. [web document] [Referred: 23.5.2023]. Available: https://metals.ovako.com/tuotteet/erikoisterakset/lastuttavuus/teraslajien-ominaisuudet/nuorrutusterakset/

Nijkerk, A.A, Dalmijn, W.L. 2004. Handbook Of Recycling Technologies. 6th Edition. Nijkerk Consultancy. Hague, Netherlands. 256 p.

SFS-ISO 262. 2010. ISO general purpose metric screw threads. Selected sizes for screws, bolts and nuts. Suomen standardisoimisliitto SFS. Helsinki. 8 p.

SFS-ISO 68-1. 2010. ISO general purpose screw threads. Basic profile. Part 1: Metric screw threads. Suomen standardisoimisliitto SFS. Helsinki. 9 p.

SFS-ISO 965-1. 2019. ISO general purpose metric screw threads. Tolerances. Part 1: Principles and basic data. Suomen standardisoimisliitto SFS. Helsinki. 22 p.

SSAB nd. Toolox® in engineering applications. [web document] [Referred: 23.5.2023]. Available: https://www.ssab.com/en/brands-and-products/toolox/product-offer/toolox-44

Suomen Autokierrätys Oy, nd. [web document] [Referred: 2.4.2023]. Available: https://autokierratys.fi/tietoa-auton-kierratyksesta/kierratysjarjestelma/romuajoneuvojen-kierratys/#materiaalit

VDI 2230. 2015. Systematic calculation of highly stressed bolted joints. Part 1: Joints

with one cylindrical bolt. Verein Deutscher Ingenieure. Düsseldorf. 182 p.

Appendix 1. Questionnaires

Questions and topics covered in interviews with shredder plant operators and maintenance personnel:

1. Have you experienced any problems with the rotor's tie bolts, such as the bolts breaking unexpectedly?

2. If you've experienced tie bolts breaking, can you identify the most common place where the breaks happen?

3. Can you recall how frequent these problems are?

4. Can you identify any other patterns to the tie bolt failures you've experienced?

5. In case of tie bolt breaking what is the maintenance protocol or repair procedure you follow?

6. Do you have an opinion on what is the most likely cause for a tie bolt breaking?

Appendix 2. Calculation model for rotor analysis

Calculation model for rotor analysis						
Universal values						
Gravity [g]		9,81	m/s^2			
Drive motor data:						
ID	Formula	Value	Unit			
Power [P]	P=T*ω	1120	kW			
Power [P]		1501,9447	hp			
Rotation speed [n]		600	rpm	=	10	1/s
Angular velocity [ω]	2*π*n	62,832	1/s			
Torque [T]	T=P/ω	17,825	kNm			
General dimensions						
ID	Formula	Value	Unit			
Radius of hammer pins [RHa]		476,5	mm	=	0,477	m
Length from pin to hammers Center of Mass [LHcm]		91	mm	=	0,091	m
Diameter of main shaft at bearing [DBe]		240	mm			
Diameter of main shaft at center [DCe]		280	mm			
Length between bearings [CCBe]		3000	mm			
Masses						
ID	Formula	Value	Unit			
Hammers in single pin [Hp]		3				
Number of pins [Ptot]		4				
Hammers in total [Ht]	Ht=Hp*Ptot	12				
Hammer mass [Mh]		90	Kg			
Rotor mass [Mr]		12000	Kg			
Total mass [Mtot]	Mtot=Ht*Mh+Mr	13080	Kg			
Static load from mass						
ID	Formula	Value	Unit			
Simplified Point load from mass [Fm]	Fm=Mtot*g/10^3	128	kN			
Static bearing load [FBe]	FBe=Mtot*g/2/10^3	64,16	kN			
Dynamic load from hard hammer contact						
Assumption: Maximum radial force generated if all hammers in a single pin make hard contact resulting in momentary spike of centrifugal forces in the opposing direction. For simplification the maximum hard contact is assumed to happen directly below rotor centerline.						
Centrifugal force at single hammer [FωH]	FωH=Mh*ω^2*(RHa+LHcm)/10^3	202	kN			
Point load from max hard contact [Fhtot]	Fhtot=FωH*Hp	605	kN			
Result						
Point loads *Fm* and *Fhtot* are working in same line but in opposing directions.						
Simplified load for simulation	Ffea=Fhtot-Fm	477	kN			
Total bearing load [FBe2]	FBe2=Ffea/2	238	kN			